Hadronic jets and jet spectroscopy in collider experiments

A. M. Moiseev
Institute for High Energy Physics, Protvino

Fiz. Elem. Chastits At. Yadra **25**, 1168–1243 (September–October 1994)

A general review is given of the data on hadronic jets obtained in experiments at e^+e^-, e^-p, and $\bar{p}p$ colliders. The phenomenological and theoretical approaches to describing the parton fragmentation mechanism and the various experimental variables used in jet analysis are discussed first. Then the algorithms for jet searches in e^+e^- annihilation are compared and some of the physical results obtained by analyzing the structure of multijet annihilation events are presented. Special attention is paid to the experiments at the CERN and FNAL $\bar{p}p$ colliders. The general features of detectors with 4π geometry and the jet search procedures are described, and the data on inclusive and multiple jet production are presented and interpreted. The preliminary experimental results obtained at the HERA collider are also reviewed; these indicate the multiple production of jets in ep interactions. It is shown that all the available experimental data are completely consistent with the predictions of perturbative QCD. The first examples of the use of the jet spectroscopy technique in collider experiments are presented, and the possibility of using jet spectroscopy for studying heavy particles at colliders of the next generation is discussed.

1. INTRODUCTION

The new theoretical ideas and experimental discoveries leading to the formulation of quantum chromodynamics (QCD) in the 1970s (Ref. 1) have considerably changed our ideas about the nature of strong interactions. However, the construction of a complete theory of hadron interactions is still far from finished even for deep-inelastic processes (DEPs), for which the most impressive results have been obtained using perturbation theory (PT) for small (at short distances) QCD coupling constant α_s. If the spacetime picture of DEPs is used as the foundation, then a sufficiently rigorous theoretical description has been obtained only for pointlike interactions (so far up to $\sim 1.4\times 10^{-17}$ cm) of partons and the evolution of separating partons up to distances of only 5×10^{-15} cm from the interaction point. However, the process of the transformation of virtual partons into the observable hadrons of the final state, which appear at distances of $(0.5–1.0)\times 10^{-13}$ cm from the interaction point, does not yet have a unique interpretation and is the subject of active theoretical and experimental research.

The main results obtained in the study of parton evolution at distances of 10^{-14}–10^{-13} cm are the discovery of hadronic jets, i.e., isolated groups of hadrons populating restricted regions of phase space, and the explanation of their production mechanism at a semiquantitative level.

In modern high-energy physics hadronic jets are, on the one hand, a new object for detection taking the place of the individual hadrons which were formerly the main object of detection in experiments at lower energies. On the other hand, it has already become apparent that the process of parton fragmentation into hadronic jets is actually related to fundamental ideas in QCD, so the detailed study of jet structure is of great interest in itself.

This review is devoted to the history of the development of this new area in high-energy physics using as examples the experimental studies at e^+e^- and hadronic (hh) colliders, where the most important results have been obtained.

2. PHENOMENOLOGICAL AND THEORETICAL APPROACHES TO THE DESCRIPTION OF PARTON FRAGMENTATION

The concept of a hadronic jet as an observable form of high-energy parton arose at the phenomenological level in the first half of the 1970s and was definitively confirmed with the completion of the basic theory of QCD. Among the stimuli which prodded physicists to develop the concept of this new hadroproduction process were the following two important ones. First, to explain the unobservability of quarks it was necessary to introduce a new form of field possessing a property which later became known as "asymptotic freedom." Second, the experimentally measured dependence $\sim p_t^{-8}$ of the hadron spectrum at large p_t instead of the dependence $\sim p_t^{-4}$ expected for hard parton scattering[2] made it necessary to assume the existence of an additional intermediate mechanism of redistribution among several hadrons of the momentum of a parton undergoing hard scattering.

One of the first to suggest the possibility that a hard parton makes a transition into a hadronic jet in a field possessing high vacuum polarizability was J. D. Bjorken. The corresponding one-dimensional problem was solved in Ref. 3 using the formalism of quantum electrodynamics, which aided the development of this idea. In particular, it was shown that after the creation of a pair of charged fermions with momenta $Q/2$, for a certain vacuum polarizability as the fermions separate the fermion charge is more and more screened by the induced charge, which after a time $t=Q/m^2$ leads to the annihilation of the initial charges with the induced charge and the production of bosons of mass m.

In that study it was concluded that in the direction of a "knocked-out" parton a jet of hadrons should appear, with the hadron multiplicity growing as the logarithm of the square of the transferred 4-momentum.

 1063-7796/94/050496-30$10.00

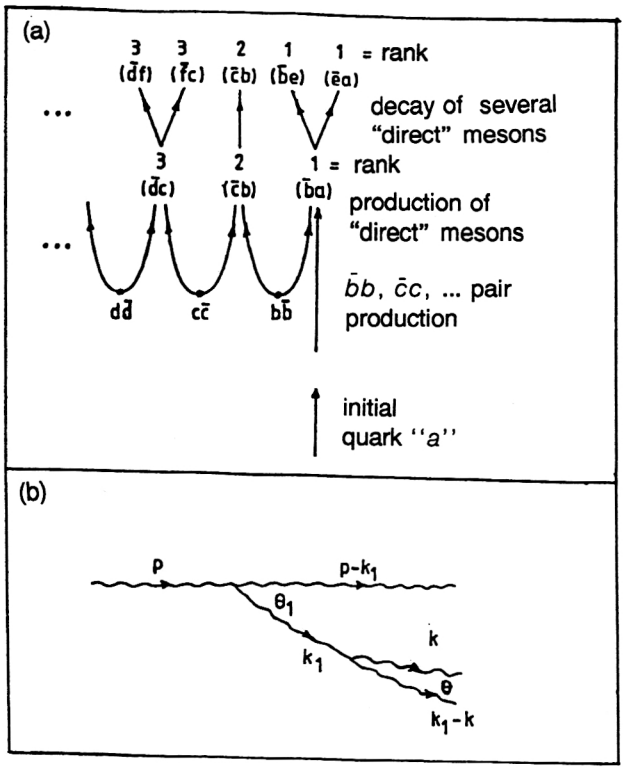

FIG. 1. (a) Schematic depiction of parton fragmentation in the FFM. (b) Schematic depiction of the gluon cascade in QCD.

2.1. Phenomenological models of independent fragmentation

Because techniques for QCD calculations were initially undeveloped, the initial attempts to describe the mechanism of distribution of the momentum of the fragmenting parton among the jet hadrons at the quantitative level were based on phenomenological models of independent fragmentation.

One of the first and most popular of these was the Feynman–Field model (FFM; Refs. 4 and 5), in which many fundamental principles of hadronic jet production by fast partons were first introduced. The development of this formalism to a level at which it could be used directly in Monte Carlo (MC) calculations and the suitable parametrization of the distribution functions introduced in the model ensured the extensive use of this model for analyzing experimental data in the first stage of research on jet production. The ideas of Feynman and Field played such an important role in establishing new ideas about hadron production mechanisms that to this day they are worth at least a brief study, although the imperfections of this model are now obvious.

The FFM is based on a simple quark–meson–quark cascade occurring owing to the successive recombination of quarks from $q\bar{q}$ pairs created in the color field of the initial quark a. The "hierarchy" of created mesons (baryons were not considered in the original FFM) is shown in Fig. 1a. According to this picture, the kinematical characteristics of the "direct" meson produced (which can be a resonance) are essentially determined by its place in the chain of successive quark–meson–quark transitions (referred to as the meson rank in Ref. 5). In that study it was assumed that in the jet produced by such a cascade the longitudinal-momentum distribution of the particles is determined by the phenomenological generating function $f(\eta)$, which gives the probability that a rank-1 meson containing the primary quark a imparts to the rest of the cascade a relative fraction of the initial momentum $\eta=1-z_1$, where $z_1=\xi_1/W_0$, ξ_1 is the longitudinal momentum of the rank-1 meson, and W_0 is the primary quark momentum. In this notation the probability that a rank-1 meson has momentum ξ_1 in the interval $d\xi_1$ will be $f(1-\xi_1/W_0)d\xi_1/W_0$, the probability that a rank-2 meson has momentum ξ_2 in the interval $d\xi_2$ will be $f(1-\xi_2/W_1)d\xi_2/W_1$, where $W_1=W_0-\xi_1$, and so on. In the end the probability for the appearance of a cascade of successively produced mesons in which the kth meson will have longitudinal momentum ξ_k in the range $d\xi_k$ can be written as

$$P(\xi_1,\xi_2,\ldots,\xi_k,\ldots)d\xi_1 d\xi_2\ldots d\xi_k\ldots=\prod_{i=1}^{\infty} f(\eta_i)d\eta_i. \tag{1}$$

where $\eta_i=\xi_i/W_{i-1}$. This leads to the recursive integral equation

$$F(z)=f(1-z)+\int_z^1 f(\eta)F(z/\eta)d\eta/\eta, \tag{2}$$

where $F(z)$ is the probability for a direct meson of any rank with relative longitudinal momentum z to appear in the quark jet.

After taking into account the various quark flavors, the experimentally observed fragmentation function $D_q^h(z)$ of primary mesons h produced in the fragmentation of this quark takes the form

$$D_q^h(z)=A_q^h f(1-z)+B^h\bar{F}(z). \tag{3}$$

In this expression the function $\bar{F}(z)$ specifying the probability for the appearance of any primary meson of rank higher than one with relative longitudinal momentum z is calculated in terms of the function $f(\eta)$, and the coefficients A_q^h and $B^h=\sum_q \gamma_q A_q^h$ are expressed in terms of the constants γ_q determining the probability of producing $q\bar{q}$ pairs of various flavors. Equation (3) can easily be generalized to take into account the production of vector resonances as primary mesons.

The following simple parametrization for light-quark fragmentation was suggested on the basis of physical considerations and analysis of the experimental data carried out in Ref. 4:

$$f(\eta)=1-a+a(b+1)\eta^b, \tag{4}$$

where a is a constant chosen in fitting the experimental data (it is usually taken to be $a=0.77$) and $b=2$. Later the function $f(\eta)=(b+1)(1-\eta)^b$, where $b=0$, 2, and 4 for c, b, and t quarks, respectively, was proposed for heavy quarks.

The meson transverse-momentum distribution is introduced into the FFM also on the basis of the assumption of local conservation of the transverse momentum in $\bar{q}_i q_i$-pair production. The absolute value of the transverse momentum of this quark and antiquark q_{ti} obeys a Gaussian distribution

$$P(q_{ti}^2)=\exp(-q_{ti}^2/2\sigma_q^2)d^2q_{ti}. \quad (5)$$

In this case all mesons of rank higher than one have the same p_t distribution with average $\langle p_t^2\rangle=2\sigma^2$, where $\sigma=\sqrt{2}\sigma_q$ (the fit to the experimental data gave $\sigma\approx 350$ MeV/c).

Experience in using the FFM to describe the inclusive spectra of particles produced in jets has shown that it correctly reproduces the main features of quark jets, especially in the region of fast particles. However, this model has a number of obvious defects. Since in it massless partons fragment into hadrons possessing a mass, energy and momentum conservation are achieved artificially after completion of the shower-modeling procedure. In addition, the FFM does not reproduce the scaling violation due to the Q dependence of the fragmentation functions.

Some of these defects of the FFM were remedied in the work of Ali *et al.*[6] on the basis of the QCD formalism. In particular, they defined a Q dependence of the function $f(\eta)$ which led to decrease of the population of the large-z region with increasing Q. In that study an attempt was made to obtain the gluon fragmentation function using the assumption that the gluon is initially converted into a $\bar{q}q$ pair.

The FFM was developed further in the work of Meyer,[7] who introduced a baryon cascade production mechanism based on diquark pair production ($qq - \overline{qq}$), which however led to the appearance in the model of additional parameters which need to be fine-tuned.

2.2. The Lund string fragmentation model

Another fragmentation model which was very popular in the 1980s was the so-called Lund string fragmentation model (LSM; Ref. 8), which was developed by theoreticians at Lund University. The LSM is based on the color confinement mechanism described above (see, for example, Ref. 3). In QCD the lines of force of the gluon field between two color charges (partons) are collimated to form a narrow color tube which can approximately be regarded as a string. In the LSM it was postulated that as the charges separate the string, whose energy is $K\approx 1$ GeV/F, is "stretched." It breaks at a charge separation of several Fermi, which leads to the appearance of $q\bar{q}$ pairs, since the energy release is sufficient to generate their mass. This corresponds to the appearance of two color strings with newly created q and $\bar{q}$ at their ends, which can in turn be stretched and break, giving rise to a parton cascade. The remaining string fragments which no longer have sufficient energy to break further correspond to ordinary hadrons. It was shown that with the assumption of a uniform energy density distribution of the field along the string this process is described by the integral equation (2) of the FFM with generating function $f(z)=1$, where $z=1-\eta$. The subsequent process of collinear gluon emission, which in the LSM formalism is represented as a "kink" in the color string, leads to the function $f(z)=z^{-1}\cdot(1-z)^c$, where $c=0.3$–0.5. The transverse momentum of the cascade partons in the LSM is modeled as in the FFM. This model possesses relativistic invariance and ensures energy and momentum conservation. Further development of this model[9] led to the introduction into it of a parton cascade stage calculated using QCD. The distinctive feature of the LSM is the appearance in it of correlations between two hadronic jets produced from a single string, for example, in e^+e^- annihilation.

The latest version of the model gives a good description of the data on e^+e^- annihilation at high energies, but it is loaded down with mathematical refinements and contains a large number of constants to be tuned.

2.3. The description of parton fragmentation in QCD

A deeper understanding of jet production mechanisms has been obtained in recent years owing to the development of techniques for perturbative QCD calculations. The most correct method for carrying out perturbative QCD calculations is to obtain the matrix elements for Feynman diagrams with increasing power of α_s. However, at present such calculations exist, with some exceptions,[10] only in next-to-lowest order PT for the emission at large angles of hard gluons which give rise to hadronic jets. For e^+e^- annihilation this corresponds to the $O(\alpha_s^2)$ approximation, which describes the final state with four partons in a configuration which allows "collinear" (due to parallel parton momenta) and "infrared" (due to parton momentum tending to zero) divergences to be avoided. The further use of the formalism of perturbative QCD to describe parton fragmentation is fraught with technical difficulties, in particular, the fact that, in addition to the initial large scale parameter Q whose introduction into renormalizable theories makes it possible to avoid the problem of divergence of integrals over Feynman diagrams containing "loops" (usually taken to be $Q \simeq \sqrt{s}/2$ for e^+e^- annihilation), smaller scale parameters arise (for example, the invariant jet mass Q_j).

Therefore, for describing the parton hadronization process special rules have been formulated for calculating a QCD cascade (jet-calculus rules) described by "branching" diagrams. These rules are based on the Altarelli–Parisi evolution equation.[11] The method was originally based on the leading-log approximation.[12]

In this approach the development of hadronic jets can be represented as a process occurring in two successive stages. In the first stage the initial parton possessing large virtual mass evolves, emitting gluons, which in turn emit gluons of the second generation and so on, until the created gluons reach sufficiently small virtual mass, which in the calculations is specified by an effective gluon evolution cutoff parameter Λ_{eff}. Gluon splitting, in which the gluon longitudinal momentum is divided asymmetrically, also dominates in this stage. As shown in Ref. 13, the cascade gluons produced are easily arranged in colorless singlets. During the second stage corresponding to "large distances" the development of the parton system concludes with hadron production, which can no longer be described using QCD. However, in the leading-log approximation the problem of "infrared" divergence remains.

Further progress in calculations of the first stage of evolution of the quark–gluon cascade was achieved after the studies of Refs. 14, 15, and 16, whose authors gave a rigorous foundation for the decrease of the gluon emission angles along each "branch" of the parton cascade owing to coher-

ence effects leading to destructive interference. This made it possible to describe quark–gluon cascades as the product of probabilities of independent parton decays into successively narrowing cones. On this basis in Refs. 14 and 15 it was shown that in the so-called doubly logarithmic approximation[17] it is possible to obtain a divergence-free expression for the matrix element of gluon multiple production in a jet by choosing the regions of phase space in which irreducible Feynman diagrams give double logarithms.

To illustrate this approach, in Fig. 16 we show part of a cascade in which a gluon with momentum p decays into gluons k_1 and $p-k_1$, after which the gluon k_1 decays into gluons k and k_1-k. In the double-log approximation $k_1>k>K$, where K is the "mass" of the gluon k. The condition of strong angular ordering of the gluons[14] arising owing to coherence of the soft bremsstrahlung requires that $\theta/\theta_1\ll 1$. In this case the probability for emitting gluon k by gluon k_1 takes the form[18]

$$P(k_1\to k)=N_c\cdot\frac{\alpha_s(k_t^2)}{\pi}\cdot\frac{dk}{k}\cdot\frac{d\theta^2}{\theta^2},$$

where N_c is the number of "colors" and k_t is the transverse momentum of the gluon k.

In Refs. 19 and 20 the inclusive spectra of partons in a jet were calculated on the basis of the rule of strong angular ordering of the gluons and it was shown that the maximum value of the rapidity distribution $y=\frac{1}{2}\cdot\ln[(E+p_L)/(E-p_L)]$ is reached for $y\approx 1/2\cdot\ln(Q/2\Lambda_{\text{eff}})$. This "peaked plateau" effect implies that in e^+e^- annihilation the inclusive hadron rapidity distribution should have a dip in the central region. The authors of Ref. 16 also obtained the well known ratio $N_g/N_q=9/4$ for the gluon multiplicities in gluon and quark jets.

However, as shown in Ref. 21, the double-log approximation, which correctly reflects the qualitative features, is inadequate for a quantitative description of a parton system with controllable accuracy. The authors of this study developed a modified leading-log approximation which completely takes into account both double-log and single-log effects in the evolution of the parton system. The gluon distribution in $\ln(1/x)$, where $x=E_g/E_j$, calculated in this approximation also manifests a peaked plateau, and for asymptotic energies in the region near the maximum it can be described by a Gaussian[22]

$$\frac{1}{\sigma}\frac{d\sigma}{d\ln(1/x)}\approx N(Y)\left(\frac{c_1}{\pi Y^{3/2}}\right)^{1/2}\exp\left[\frac{-c_1((\ln(1/x)-\ln(1/x_0))^2}{Y^{3/2}}\right],\tag{6}$$

with maximum at $\ln(1/x_0)=(Y/2)+c_2\sqrt{Y}+O(1)$, where $c_1=\sqrt{36N_c/b}$; $c_2=B\sqrt{b/16N_c}$; $Y=\ln(Q/2\Lambda_{\text{eff}})$; $b=(11N_c/3)-(2N/3)$; $B=(1/b)[(11N_c/3)+(2N_f/3N_c^2)]$; N_c and N_f are the number of colors and flavors, respectively. The term $O(1)$ describes higher-order corrections and for $Q\to\infty$ it should be constant. The factor $N(Y)$ corresponds to the calculated gluon multiplicity at the end of the cascade. It has been proposed on the basis of local parton–hadron duality[23] that it corresponds to the hadron multiplicity up to a normalization factor $K(Y)$.

The inclusion of higher-order perturbative corrections done in Ref. 24 showed that the distribution in $\ln(1/x)$ deviates from a Gaussian and includes two higher moments

$$s=\langle(\xi-\bar{\xi})^3\rangle/\sigma^3,\quad k=\langle(\xi-\bar{\xi})^4\rangle/\sigma^4-3,$$

in the form

$$\frac{1}{\sigma}\frac{d\sigma}{d\ln\xi}=\frac{N(Y)}{\sqrt{2\pi}}\exp\left[\frac{k}{8}-\frac{s\delta}{2}-\frac{(2+k)\delta^2}{4}+\frac{s\delta^3}{6}+\frac{k\delta^4}{24}\right],\tag{7}$$

where $\delta=(\xi-\bar{\xi})/\sigma$, $\sigma=\langle(\xi-\bar{\xi})^2\rangle^{1/2}$, and $\xi\equiv\ln(1/x)$.

A number of other specific predictions for various kinematical regions of the parton cascade have also been obtained in perturbative QCD. For example, at small x with the condition of strong ordering in x_i (i.e., $x_1\gg x_2\gg\ldots x_n$), but without significant restrictions on $k_{t_i}^2$, the authors of Refs. 25 and 26 obtained a different asymptotic solution for gluon multiple production, which indicates the possible appearance of "hot spots," i.e., regions of phase space limited in k_t with very high gluon density $[dn/d\ln(1/x)\sim 1/\alpha_s]$, with the gluons interacting with each other in rapidity space at distances of order unity.[27]

The authors of Ref. 28 have performed calculations for the two-particle correlation function $R(x_1,x_2,Q)$ indicating the existence at small x_i of positive short-lived correlations due to coherent gluon emission. However, the results of the calculations proved to be very sensitive to corrections to the leading-log approximation and therefore are actually semiqualitative.

All the results mentioned here pertain to light-quark fragmentation. The QCD analysis of heavy-quark fragmentation has predicted significant differences in the cascade-gluon spectra. In particular, soft gluon emission is suppressed in this case, and a "dead cone" appears in the region $x\to 1$ (Refs. 28 and 29).

We conclude this section by noting that, on the whole, the technique of calculating the evolution of gluon systems using perturbative QCD has already reached an accuracy sufficient for experimental verification at the quantitative level.

3. PROGRAMS FOR THE MONTE CARLO MODELING OF PROCESSES INVOLVING JET PRODUCTION

As shown in the preceding section, the process of parton transformation into hadronic jets is probabilistic in nature, so it is appropriate to use the Monte Carlo method to calculate various jet characteristics at a level allowing direct comparison with experimental results. However, in general, such comparison requires the jet production mechanism to be taken into account. This problem can be solved relatively simply only for low-energy e^+e^- annihilation. However, the correct representation of deep-inelastic lepton–hadron and hadron–hadron collisions is just as difficult computationally as describing post-interaction parton fragmentation, since it must include a picture of the evolution of the initial partons.

Therefore, to obtain theoretical predictions for hard processes accompanied by jet production, work began in the 1980s on writing computer superprograms which completely reproduce all the details of the theoretical description of such processes known at a given time.

These programs are usually supported and constantly revised by a group of authors, so that there is an entire series of different versions of them. Here we shall describe recent versions of some of these programs.

3.1. The ISAJET program

One of the first programs of this type is ISAJET (Ref. 30), created at Brookhaven National Laboratory (USA) for the MC modeling of hard subprocesses in pp and $\bar{p}p$ collisions. The ISAJET calculations of all the related effects are organized in the following stages.

3.1.1. First, hard-interaction subprocesses are simulated. These include parton two-particle scattering, single and pair production of vector gauge bosons, creation of supersymmetric particles, and so on.

These calculations are performed in lowest-order perturbative QCD.

3.1.2. The evolution of the produced partons is described up to $\Lambda_{\text{eff}}=6$ GeV using the leading-log approximation of QCD (Ref. 31) neglecting coherence effects. The final hadronization of the final-state partons is realized using the FFM with $\langle q_t \rangle = 0.35$ GeV/c.

3.1.3. Gluon emission by the primary parton with space-like virtual mass is modeled by ISAJET using the method proposed in Ref. 32, where the evolution of the initial parton is done in the reverse direction after the hard interaction of partons of the needed type at maximum Q^2 with the virtual masses of the emitted gluons ordered by hand.

This program has been used extensively to analyze the experimental data at existing $\bar{p}p$ colliders. On the whole it has provided a good description of these data, but for the process $\bar{p}p \to W+n(\text{jet})$ at $\sqrt{s} = 1.8$ TeV it has been found that ISAJET significantly underestimates the cross sections for $n \geqslant 2$ (Ref. 33).

3.2. The HERWIG program

This program[34] has been designed by a collaboration headed by B. R. Webber at Cambridge University. He is one of the most active theoreticians working on developing QCD, and from the theoretical point of view this is one of the most complete of all programs of this type. The HERWIG program is primarily distinguished by its systematic inclusion of coherence effects,[1)] and it incorporates the basic forms of DEPs.

3.2.1. In the modeling of hard lepton–lepton, lepton–hadron, and hadron–hadron processes this program includes the color structure of the subprocess, since the interference of the gluons emitted from different color configurations restricts the phase space for the first soft gluon emitted by a hard parton.[35] This causes the size of the cone for the first emission of a gluon by a parton i to depend on the emission angle of its color partner j.

3.2.2. The final-state parton evolution is modeled taking into account coherence effects in the form of strong angular ordering, as described in Sec. 2.3. The program also includes the azimuthal correlations between jets arising both from interference effects and from gluon polarization. After the modeling of the gluon cascade each gluon gets a virtual mass Q_g (which must be greater than twice the light-quark mass) and gluons are converted into $\bar{q}q$ pairs. Colorless "preclusters" with an average mass of about $3Q_g$ are formed from these quarks. If such a precluster is too light to decay into two hadrons, it gets the mass of the lightest hadron with the given quark content. Heavier preclusters decay into two hadrons or cascade-fashion into a larger number of hadrons. The program includes the possibility of gluon decay into diquarks and processes of heavy (b and t) quark production.

3.2.3. The evolution of the initial partons in the HERWIG program is modeled on the basis of the rules formulated in Ref. 34. In particular, the quantity $Q_i = E_i\sqrt{\xi_i}$ is used as the cascade variable for a space-like cascade; here $\xi_i = \vec{p}\times\vec{q}_i/E\omega_i$, and $\vec{p}$, E and $\vec{q}_i$, ω_i are the 3-momenta and energies of the cascading and emitted partons. The evolution of the primary hadrons is modeled in the reverse direction after simulation of a hard subprocess.

The HERWIG program is widely used to interpret the data from experiments at e^+e^- and hh colliders.

3.3. The JETSET program

This program was designed specially for describing multijet events in e^+e^- annihilation.[36] It uses an algorithm for parton cascade development which includes coherence effects with additional constraints such that hard-gluon emission at large angles occurs according to a prescribed matrix element calculated in second-order perturbative QCD. The parton cascade development in JETSET ends at $\Lambda_{\text{eff}} \simeq 1.5$ GeV, and the hadronization of the produced partons is treated using the LSM.

There is a series of similar programs (COJET,[37] EUROJET,[38] and so on) which differ from the programs described above in the details of the algorithms for modeling parton cascades and which use one of the fragmentation schemes described above.

4. JET PRODUCTION IN e^+e^- ANNIHILATION

The cleanest conditions for studying hadronic jets occur in e^+e^- annihilation into two quarks

$$e^+e^- \to q\bar{q}, \tag{8}$$

so the first experiments to seek hadronic jets and study their characteristics were carried out in e^+e^- colliding beams. However, at the relatively low energies of the e^+e^- storage rings existing in the middle 1970s it was practically impossible to experimentally detect individual jets even in the reaction (8). Since in the quark-parton model events of reaction (8) should have two hadronic jets in opposite directions, for detecting this effect and measuring the direction of the jet axis methods were developed for analyzing the shape of the event as a whole using so-called collective variables. This approach was later used to analyze events of more complicated form, which lead to a wider range of collective variables. Below we shall consider the most useful ones.

4.1. Collective variables

The first of the variables used to analyze the shape of an event in phase space were those used to describe axially symmetric events. These are the sphericity and the thrust,[39,40] defined as

$$S=\left(\min \sum_{i=1}^{N}(p_t^i)^2\right) \Big/ \sum_{i=1}^{N}(p^i)^2,$$

$$T=\left(\max \sum_{i=1}^{N}(|p_L^i|)\right) \Big/ \sum_{i=1}^{N} p^i,$$

where the summation runs over all charged particles, p_t^i is the transverse momentum relative to the axis for which $\Sigma_{i=1}^{N}(p_t^i)^2$ has the minimum value, and p_L is the longitudinal momentum of a particle relative to the axis for which $\Sigma_{i=1}^{N}|p_L^i|$ has the maximum value. For two-jet events S tends to zero and T to unity as the jet narrows; for completely spherical events $S=1$ and $T=0.5$. The axes determined by calculating S and T are a good approximation to the axes of a two-jet event.

A defect of the variable S is the impossibility of computing it exactly in QCD owing to the "infrared" divergence. Therefore, the T distributions are used for comparison with QCD predictions.

The sphericity tensor made up of the components of the momenta of all secondary particles i has been proposed for analyzing events of more complicated shape:[39,41]

$$M_{\alpha\beta}=\sum_{i=1}^{N} p_\alpha^i p_\beta^i, \quad \alpha,\beta=x,y,z,$$

which is diagonalized for each event. The eigenvectors $\vec{n}_j$ and associated eigenvalues λ_i of this tensor are sometimes referred to as the "principal axes" of the event. The normalized eigenvalues

$$Q_j=\lambda_j/\sum_{j=1}^{3}\lambda_j$$

when ordered as $Q_1<Q_2<Q_3$ respectively denote the thickness, width, and length of the event. In this notation $S=\frac{3}{2}(Q_1+Q_2)$. In addition to the sphericity, other possible independent-variables are the planarity

$$P=(Q_2-Q_1)$$

and the flatness of an event

$$F=1-Q_1/Q_2,$$

which for flat events has the value $F=1$.

A quantity sometimes used which is equivalent to the sphericity variable and whose distribution can be compared to QCD calculations is the spherocity,[42] which has a somewhat more complicated definition.

Using the "principal-axis" method it is possible to find the deviation of the shape of an event from a two-jet configuration, but here the vector $\vec{n}_3$ gives the direction of only the event axis averaged over more than two jets. In order to determine the axis of each of the three possible jets a special method[43] was developed which already approaches the algorithms for finding each jet individually. In this method all the final-state particles with 3-momenta $\vec{p}_1,\vec{p}_2\ldots\vec{p}_N$ are grouped in three nonempty subsets C_1,C_2,C_3 with total 3-momenta $\vec{P}(C_l)\Sigma_{i\in C_l}=p_i$, $l=1,2,3$. These vectors are used to construct a variable called the triplicity

$$T_3=\left(1 \Big/ \sum_{i=1}^{N}\left|p_i\right|\right)\max_{C_1,C_2,C_3}\{|\vec{P}(C_1)| + |\vec{P}(C_2)|+|\vec{P}(C_3)|\}.$$

This variable has value $T_3=1$ for configurations of three isolated jets and $T_3=3\sqrt{3/8}=0.65$ for completely spherical events. The subsets C_i^* ensuring the maximum value of T_3 are identified as hadronic jets having 3-momenta $\vec{P}(C_i)$. Owing to momentum conservation, these vectors must be coplanar. The angles between the jets in this "triplicity plane" can be interpreted as the angles between partons.

For determining the shape of more complicated events, the authors of Ref. 44 proposed variables usually referred to as the Fox–Wolfram moments:

$$H_l=\sum_{i,j}\frac{|\vec{p}_i||\vec{p}_j|}{s}\cdot P_l(\cos\varphi_{ij}),$$

where the summation runs over all the particles of each event, P_l is a Legendre polynomial, and φ_{ij} is the angle between the 3-momenta of particles i and j. The even moments are used to describe the shape of symmetric events, and the odd ones reflect the degree of asymmetry of an event. In particular, for spherical events all the moments with $l\geqslant 2$ are equal to zero, and events with two collinear jets give $H_l=1$ for even l and $H_l=0$ for odd l. For symmetric three-jet events the moments H_2 and H_3 have the maximum values 1/4 and 5/8, respectively.

The authors of Ref. 45 considered a more general invariant method of distinguishing multijet events in the space of four-dimensional relative velocities $u_i=p_i/m_i$, where p_i are the particle 4-momenta and m_i are their masses. However, this method has not yet been used for analyzing the experimental data in collider experiments.

In studies at e^+e^- colliders at large $\sqrt{s}$ and particularly in experiments at hh colliders it is necessary to isolate events containing jets with large transverse momenta. However, at detectors with 4π geometry in colliding beams only the angles and energy of such jets are measured using sectioned calorimeters. Therefore, the concept of the transverse energy $E_{ti}=E_i\sin\theta_i$, where θ_i is the emission angle of particle i relative to the beam axis, has been introduced, and a new collective variable, the total transverse energy of the event ΣE_{ti}, has been defined. For seeking events with hard neutrinos (from heavy-particle decays) it has become usual to use a collective variable referred to as the missing transverse energy:

$$E_t^{\text{missing}}=\left[\left(\sum E_{ti}\cos\varphi_i\right)^2+\left(\sum E_{ti}\sin\varphi_i\right)^2\right]^{1/2},$$

where φ_i is the azimuthal angle of particle i. This variable serves as a measure of the imbalance in the transverse momentum.

4.2. The detection of quark and gluon jets

The first data on the jet structure of hadronic final states in e^+e^- annihilation were obtained using the SLAC–LBL magnetic spectrometer at the SPEAR storage rings and were published in 1975 (Ref. 46). In this experiment it was shown that as the total c.m. energy $\sqrt{s}$ increases from 3.0 to 7 GeV the quantity $\langle S \rangle$ significantly decreases. Confirmation of the theoretical prediction that the quark spin is 1/2 was first obtained from the distribution in the angle between the axes of two-jet events and the colliding-beam axis, which corresponds to the angular distribution of $q\bar{q}$-pair emission. These important data, which were later refined in experiments at the PETRA $e^{\pm}$ storage rings for $\sqrt{s}$ in the range from 14 to 34 GeV, were in good agreement with the main ideas of the quark–parton model, which associated the constituents of the static quark model with the partons observed in deep-inelastic scattering experiments.

Even more fundamental results were obtained at the PETRA storage rings in 1979, when events with three jets were first distinguished in all four experimental setups located at the e^+e^- intersection points in this collider.

It is interesting to observe that the first hints of the existence of three-jet events came from the visual scanning of the angular distributions of the energy flux. To quantitatively confirm the presence in high-energy multihadron e^+e^--annihilation events of a third jet corresponding to a gluon emitted by one of the quarks of a $q\bar{q}$ pair, in the PETRA experiments the distributions in certain collective variables were compared with the results of calculations using the quark-parton model for the process (8) and the QCD calculations for the process

$$e^+e^- \to q\bar{q}g. \tag{9}$$

In Fig. 2 we show the distribution in the planarity P for multihadron events recorded by the JADE detector[47] at $\sqrt{s}=27.7$ and 30 GeV. It follows from this that calculations using the quark–parton model with the value of σ_q, which determines the distribution in the transverse momentum q_t of the quarks in the hadronization cascade according to the FFM (see Sec. 2.1), even significantly greater than the value $\sigma_q=250$ MeV/c found at low energies cannot reproduce these experimental data. Conversely, the QCD calculations for reaction (9) are in good agreement with the experimental results.

In the experiment at the PLUTO detector[48] after the selection of multihadron events according to the value of the thrust T assuming that the events are two-jet ones, the jets were classified as narrow (with smaller $\langle p_t \rangle$) and broad (with larger $\langle p_t \rangle$). In such a selection an additional gluon jet can form part of a broad jet. In fact, it was shown that the weak energy dependence of $\langle p_t^2 \rangle$ for narrow jets observed in the range 13–30 GeV is reproduced well by both the quark–parton model and QCD, but the more significant increase of $\langle p_t^2 \rangle$ observed for broad jets arises only in QCD as a result of

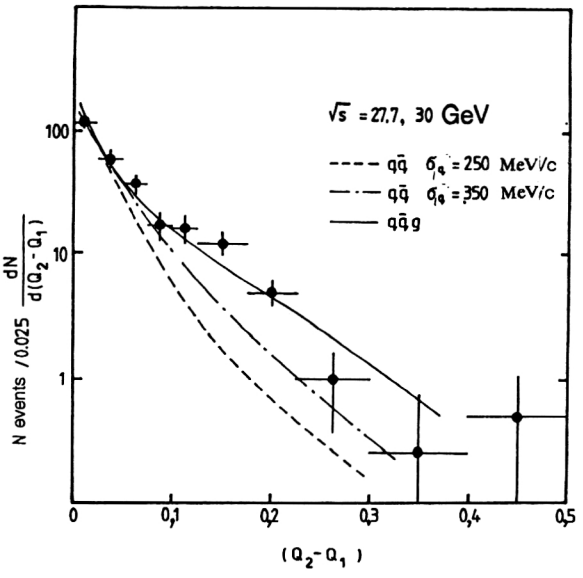

FIG. 2. Distribution in the planarity $P=Q_2-Q_1$ of multihadron events from e^+e^- annihilation at $\sqrt{s}\approx 30$ GeV. The dashed and dot-dashed lines correspond to the FFM results, and the solid lines show the QCD results for the process (9).

emission of a bremsstrahlung gluon by one of the quarks. In this experiment events with markedly three-jet configurations were selected by means of cuts in the triplicity T_3, the thrust T, and the sphericity S. The number of such events is in good agreement only with the QCD calculations for reaction (9). Similar results confirming that at high energies in e^+e^--annihilation events a third parton appears which can be identified with the gluon predicted by QCD have been obtained using the TASSO (Ref. 49) and MARK-J (Ref. 50) detectors.

However, for definitive confirmation of the fundamental prediction of QCD regarding the existence of gluon fields it was necessary to obtain experimental proof that the spin of the third parton appearing in e^+e^- annihilation is equal to unity. Therefore, in the early 1980s many studies were carried out of the possibility of determining the gluon spin in high-energy e^+e^- annihilation.[51–54] In particular, in Ref. 51 it was shown that the distribution in $\cos\tilde{\theta}$, where $\tilde{\theta}$ is the angle in the plane of a three-jet event between the direction of the jet with maximum energy and the direction of the two other jets in their rest frame depends significantly on the value of the gluon spin. In Fig. 3 we show the distribution in $\cos\tilde{\theta}$ obtained in Ref. 55 using data from the TASSO detector for the energy range $27.4<\sqrt{s}<36.6$ GeV. In this study "collective" variables were use to carefully select 248 three-jet events with relative energy of the hardest jet $x_1=E_1/E_{\text{beam}}<0.9$. The results of the first-order perturbative QCD calculations shown in Fig. 3 and the analogous calculations using the scalar-gluon model[56] show that the first version is clearly favored. Even more convincing proof that the gluon spin is unity was obtained by comparing the experimental value $\langle\cos\tilde{\theta}\rangle_E=0.349\pm0.013$ with the calculated values $\langle\cos\tilde{\theta}\rangle_V=0.341\pm0.004$ and $\langle\cos\tilde{\theta}\rangle_s=0.292\pm0.003$.

The theoretical calculations carried out in Ref. 52

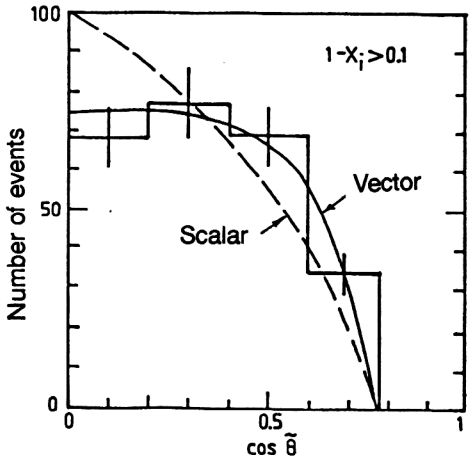

FIG. 3. Distribution in cos $\tilde{\Theta}$ for three-jet events from e^+e^- annihilation at $\sqrt{s}=30$ GeV. The solid line shows the QCD calculations and the dashed line shows the calculations using the model with scalar gluon.

showed that the value of the gluon spin also affects the shape of the x_1 distribution. The analysis of this distribution in the range $0.7<x_1<0.95$ carried out in Ref. 57 using data from the PLUTO detector at energies of about 30 GeV confirmed the fact that the hypothesis that the third jet has spin $s=1$ is the most probable. The physicists working at the CELLO detector at the energy $\sqrt{s}=34$ GeV later arrived at the same conclusion.[58]

4.3. Algorithms for isolating individual hadronic jets at intermediate energies

Although the use of collective variables for analyzing e^+e^- interactions made it possible to effectively distinguish two- and three-jet events and to obtain fundamental physical results providing important experimental confirmation of the correctness of the main ideas of QCD, by the beginning of the 1980s the possibilities offered by this technique for processing the experimental data had largely been exhausted.

To check the predictions of QCD further it was necessary to obtain data on annihilation events involving four and more jets, and to check parton fragmentation models it was necessary to carry out a detailed study of the structure of single jets. Moreover, the energy $\sqrt{s}\simeq 35$ GeV reached at the PETRA storage rings already ensured that the hadronic jets were well separated in the detector, which made it possible to pose the question of the isolation of individual jets by means of special algorithms.

One of the first to be proposed was the "angular" jet algorithm,[59] in which a jet is isolated using the fact that the parton fragmentation products are collimated relative to the direction of the parton momentum. This algorithm includes the following steps:

• First the fastest particle is picked out, and all the other particles in the angular range $\Delta\theta<\alpha$ are added to it, forming a "precluster." A similar operation is performed successively for all the other particles. The direction of the precluster axis is obtained by summing the 3-momenta of all the particles involved in it.

• All preclusters with angles between their axes less than $\Delta\theta=\beta$ are combined into clusters, and their energies and 3-momenta are determined by summing those of all the particles involved in them.

• Clusters with $E_{\text{cl}}\geqslant E_{\min}$ and $n_{\text{part}}\geqslant n_0$ are assumed to be jets.

• All the jets in an event are assumed to be correctly identified if the condition $\sum_{i=1}^{n_c} E_{\text{cl}} > E_{\text{vis}}(1-\epsilon)$ is satisfied, where $\epsilon\ll 1$ is the part of the energy E_{vis} deposited in the detector which can belong to particles not forming part of the jet.

This relatively simple algorithm has been used as an additional method of distinguishing three-jet events in some of the studies on the gluon spin referred to above. For example, in Ref. 57 it was used successfully with the following parameter values: $\alpha=30°$, $\beta=45°$, $E_{\min}=2$ GeV, and $\epsilon=0.1$.

The technique of distinguishing jets on the basis of restrictions of the "relative differences" of the kinematical variables of the particles involved in the jet has been actively developed further. One example of this approach is the LUCLUS algorithm,[60] in which particles with relative transverse momentum not exceeding a specified value are combined to form a jet.

However, until recently the type of algorithm first proposed by the JADE Collaboration has been most practical for application in studies of e^+e^- interactions. This is related to the fact that perturbative QCD calculations in $O(\alpha_s^2)$ have been performed only for massless partons. Therefore, when it is necessary to directly compare the data with analytic QCD calculations, for experimental jet selection it is necessary to use an algorithm which could also be used for performing the corresponding operations in calculations involving massless partons in QCD.

The original JADE algorithm[61] is organized as follows:

• First the invariant masses m_{ij} of all pairs of "particles" in the selected event are calculated. Here a "particle" can be a real particle which hit a single cell of the calorimeter or a "pseudoparticle," defined below. The invariant mass is calculated assuming that particles i and j have zero mass

$$m_{ij}^2=2E_iE_j(1-\cos\theta_{ij}),$$

and the energy and 3-momentum of the pair are obtained by adding these quantities for the individual particles

$$E_{ij}=E_i+E_j$$

$$\vec{P}_{ij}=\vec{P}_i+\vec{P}_j.$$

• The invariant mass m_{ij} calculated in this manner is used to determine the dimensionless quantity

$$y_{ij}=\frac{m_{ij}^2}{s},$$

sometimes referred to as the "jettiness," where s is the square of the total energy in the c.m. frame.[2)]

The pair of particles with the smallest value of y_{ij} is called a pseudoparticle, and these two particles are replaced by such a pseudoparticle in the rest of the analysis.

• The procedure is repeated until all the y_{ij} begin to exceed some maximum value y_{cut}.

• All the pseudoparticles produced in this stage are assumed to be jets.

However, algorithms of this type possess an ambiguity, often referred to as the "recombination-scheme uncertainty," because the results obtained significantly depend on the details of the procedure for redefining the kinematical variables used to ensure that the final-state hadrons combined to form the jet are similar to the massless partons in the QCD calculations.

By now several recombination schemes have been studied in order to find the one for which the analytical perturbative QCD calculations in $O(\alpha_s^2)$ are most suitable for direct comparison with the experimental data, i.e., the one for which the hadronization corrections are sufficiently small. The main ones are the E, EO, P, and PO schemes.[62] They differ from each other in how the pseudoparticle 4-momentum is formed from the 3-momenta and energies of the initial particles (or pseudoparticles).

However, the increasing accuracy of experiments at e^+e^- colliders and the improvement of techniques for perturbative QCD calculations revealed defects in this approach. The main one is the possibility of forming a pseudojet from soft bremsstrahlung gluons, which should actually be included in the jets associated with the partons emitting these gluons. In fact, for $E_i \ll \sqrt{s}$ and $E_j \ll \sqrt{s}$ the value of y_{ij} can be a minimum even when particles i and j are produced in the fragmentation of soft gluons emitted by different partons, and their 3-momenta are separated by a rather large angle. The production of such soft pseudojets cannot be taken into account sufficiently accurately in second-order perturbative QCD calculations, which means that for small y_{ij} there are large corrections from higher orders. Therefore, several new algorithms have been proposed for isolating jets in e^+e^--annihilation events which would preserve the weak dependence on the hadronization model present in algorithms of the JADE type, but which would make it possible to decrease the corrections from higher orders for the corresponding QCD calculations.

The most successful of these proved to be the k_t or the Durham algorithm,[63] in which the sequence of operations of the JADE algorithm is retained, but the relative transverse momentum rather than the invariant mass is used as the variable on which the jet isolation is based. The jettiness in the k_t algorithm is defined as

$$y_{ij}=2(1-\cos\Theta_{ij})\min(E_i^2,E_j^2)/s,$$

which for small Θ_{ij} corresponds to the minimum transverse momentum in the jet. The use of this algorithm makes it easy to include higher-order corrections in perturbative QCD calculations and to avoid the problems of pseudojets of soft particles emitted at large relative angles.[64] Detailed study of this scheme for modeled events has shown that it has advantages compared to the algorithms used earlier, at least in the calculation of the cross sections for annihilation events at small y_{ij}.

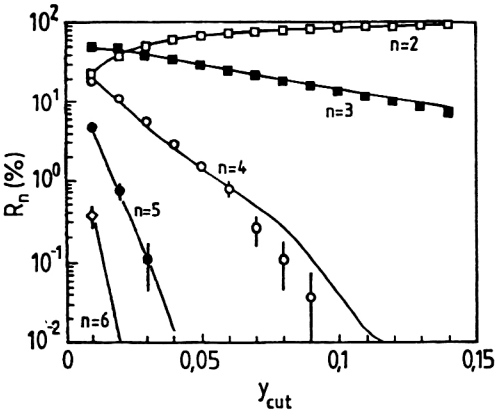

FIG. 4. Dependence on y_{cut} of the relative cross sections R_n for multijet production in e^+e^- annihilation at $\sqrt{s}=54-61.4$ GeV. The curves show the results of analytic QCD calculations.

4.4. Cross sections for events with several jets

The technique described above for experimentally distinguishing individual jets in e^+e^- annihilation events ensures the possibility of correctly comparing the results of QCD calculations with experimental estimates of the relative cross sections $R_n=\sigma_n/\sigma_{\text{tot}}$, where σ_{tot} is the total cross section for e^+e^- annihilation into hadrons and σ_n is the cross section for annihilation interactions leading to the production of n jets in the final state. Actually, in the $O(\alpha_s^2)$ approximation of perturbative QCD the quantities R_n can be represented as an expansion in powers of $\alpha_s(\mu)$ (Ref. 65):

$$\begin{aligned} R_2&=1+C_{2,1}(y_{\text{cut}})\cdot\alpha_s(\mu)+C_{2,2}(y_{\text{cut}},f)\cdot\alpha_s^2(\mu),\\ R_3&=C_{3,1}(y_{\text{cut}})\cdot\alpha_s(\mu)+C_{3,2}(y_{\text{cut}},f)\cdot\alpha_s^2(\mu),\\ R_4&=C_{4,2}(y_{\text{cut}})\cdot\alpha_s^2(\mu), \end{aligned} \tag{10}$$

where μ is the renormalization scale at which α_s is defined and $f=\mu^2/s$.

Here

$$\alpha_s(\mu)\simeq\frac{12\pi}{(33-2\times N_f)\cdot\ln(\mu/\Lambda_{\overline{MS}})^2},$$

and $\Lambda_{\overline{MS}}$ is the QCD scale constant, found from experiment.

The coefficients $C_{n,k}$ incorporating the explicit dependence on y_{cut} can be calculated in perturbative QCD for different recombination schemes.

In Fig. 4 we show the y_{cut} dependence of the cross sections R_n measured at the TRISTAN e^+e^- collider at energies $\sqrt{s}=54-61.4$ GeV (Ref. 66), isolated using the JADE algorithm. We see that even at such high energies it is impossible to uniquely determine the absolute values of R_n, since they depend strongly on y_{cut}, especially for $n\geqslant 3$. However, this should not be considered a defect of this algorithm, since the introduction of a y_{cut} dependence of R_n is one of the methods of resolving the real ambiguity in jet definition related to the presence in jets of soft hadrons emitted at large angles to the jet axis. This approach makes it possible to avoid a number of complicated methodological problems such as jet overlap and background from events with incor-

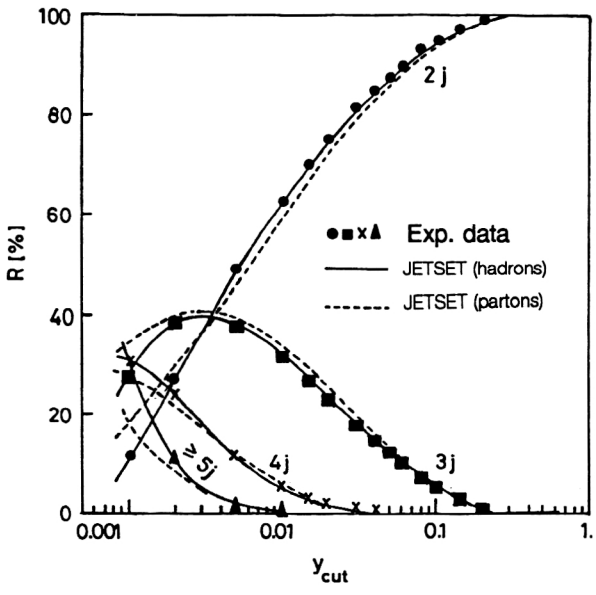

FIG. 5. Dependence on y_{cut} of the relative cross sections R_n for multijet production in e^+e^- annihilation at $\sqrt{s}=91$ GeV obtained at the OPAL detector. The curves show the results of calculations using the JETSET program.

rectly determined jet multiplicity, and it ensures the solution of many physical problems. Actually, the results of the $O(\alpha_s^2)$ perturbative QCD calculations shown in this figure, which include the parton hadronization process and also detector-related effects, give a good description of the experimental data on R_n in a wide range of y_{cut} after optimization of the value of $\alpha_s(\mu)$.

The most careful measurements of R_n have been made at the LEP e^+e^- collider at $\sqrt{s}=M_{Z^0}$. In Fig. 5 we show the y_{cut} dependences of R_n obtained at the OPAL detector[67] using the k_t algorithm, which made it possible to compare the results with the QCD calculations for values of y_{cut} considerably smaller than in Fig. 4. The curves shown in Fig. 5 were calculated using the JETSET program. The dashed lines show the results of the calculations performed at the parton level, and the solid lines show the results of calculations at the hadronization level. It follows from these data that the hadronization corrections are important only for $y_{cut}<0.003$. Comparison of these results with those obtained earlier on the basis of recombination schemes for the JADE algorithm[68] indicates that the k_t algorithm leads to smaller corrections for hadronization.

4.5. Some results obtained in the study of multijet events

As shown in Sec. 4.2, the isolation of three-jet events and study of their structure led to the discovery of the vector nature of the gluon. Further study of multijet events at the e^+e^- colliders TRISTAN, SLS, and LEP made possible the detailed experimental verification of calculations including higher orders of perturbative QCD. However, the analysis of all the physical results obtained at these colliders lies outside the scope of this review, and here as an example we shall give the results of measurements of a number of fundamental QCD constants.

4.5.1. Measurement of α_s

Among the numerous ways of experimentally determining α_s (see, for example, the review of Altarelli[69]), one of the most accurate is measurement of this quantity from the ratio of the yields of three- and two-jet events. Actually, first-order perturbative QCD calculations give α_s/π for this ratio. The inclusion of second-order terms leads to Eq. (10), which is used for the more accurate determination of the QCD scale constant $\Lambda_{\overline{MS}}$.

At all the experimental setups at LEP except for L3, the method proposed by the OPAL Collaboration[70] was used to determine the constant $\Lambda_{\overline{MS}}$. In this method the differential distribution

$$D(y)=\frac{R_2(y)-R_2(y-\Delta y)}{\Delta y},$$

is measured, where $y=y_{cut}$, where the event classification changes from three-jet to two-jet. The first series of measurements of $\Lambda_{\overline{MS}}$ were made using the various recombination schemes of the JADE algorithm. Although the experiments carried out at different LEP setups (Refs. 70–73) differed in many details of their analysis (in particular, some were carried out only with charged and neutral hadrons separately, while others used them together), they gave consistent results. Averaging over the four experiments gave the value $\alpha_s(M_{Z^0}) = 0.119 \pm 0.008$. However, it turned out that the quantity $\Lambda_{\overline{MS}}$ determined in this way significantly depends on the renormalization parameter μ, and its value obtained from a fit to the experimental data was too small. For example, according to the OPAL data,[70] the value of $\Lambda_{\overline{MS}}$ found as a result of approximating the $D(y)$ distribution at the fixed value $f=1$ turned out to be 330 MeV, while when $\Lambda_{\overline{MS}}$ and f were determined jointly the values 147 MeV and 0.0052, respectively, were obtained. The existence of this dependence of $\Lambda_{\overline{MS}}$ on the scale parameter indicated the necessity of including higher-order terms in the perturbative QCD calculations. Further analysis showed that a lower value of μ resulted from a fit of the data at small y_{ij}, where the perturbative QCD calculations were least accurate, because the form of the variable y_{ij} in the JADE algorithm did not permit use of the technique of resumming the leading-log terms.[74,75] This defect was eliminated by going to the k_t algorithm, which permits resummation for small y_{ij} not only of the leading-log terms, but also of all the higher-order terms. Processing of the OPAL data using the k_t algorithm[67] led to the values $\Lambda_{\overline{MS}} = 244^{+19}_{-13}$ and $f=0.25$. After such reprocessing of the data from the other LEP detectors the new average value became $\alpha_s(M_z)=0.123\pm0.005$ (Ref. 69), which, however, coincides with the earlier value within one standard deviation.

Another source of systematic discrepancy in comparing the experimental data and the analytic QCD calculations is the effect of the hadronization process, which can be included only on the basis of MC calculations. As a result of such calculations it was shown that for the EO scheme the

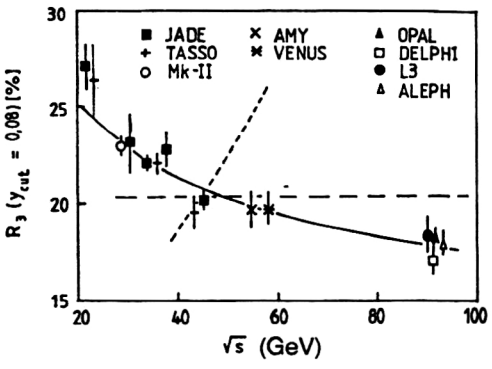

FIG. 6. Energy dependence of the coupling constant α_s calculated from R_n. The solid line shows the results of analytic calculations in lowest-order perturbative QCD, the dashed line corresponds to α_s=const, and the dotted line shows the energy dependence of the coupling constant α_A in the Abelian vector theory.

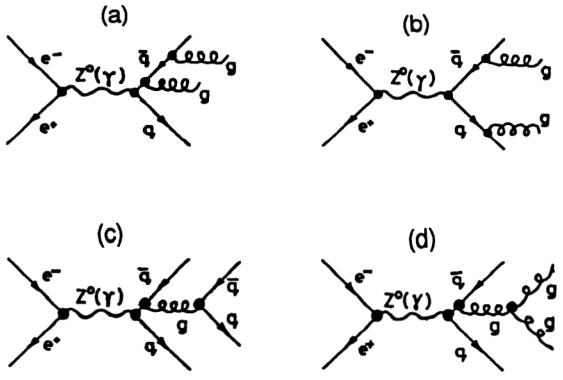

FIG. 7. Feynman diagrams describing the production of 4-jet events in e^+e^- annihilation.

uncertainty in measuring the relative yields of events with different numbers of jets due to the hadronization process was less than $\pm 2\%$ for $\sqrt{s}$ in the range from 25 to 100 GeV. Therefore, study of the energy dependence of the cross sections for events with n jets at fixed y_{cut} is a reliable method of determining the energy dependence of α_s. In Fig. 6 we show the data on $R_3(y_{\text{cut}}=0.08)$ for $\sqrt{s}$ in the range from 22 to 91 GeV (Ref. 76), obtained at the PETRA, PEP, TRISTAN, and LEP colliders using the EO recombination scheme, which permits them to be compared with analytic perturbative QCD calculations at order $O(\alpha_s^2)$. The solid line in Fig. 6 corresponds to the results of approximating the experimental data by the analytic expression for R_3 with scale coefficient $f=1$. The dashed line in this figure corresponds to the hypothesis that the constant α_s is independent of the energy. These data suggest that the existing experimental results reliably exclude the hypothesis that α_s is independent of the energy, while the same results are well described by the $O(\alpha_s^2)$ approximation of perturbative QCD, which is convincing evidence in favor of a "running" α_s, i.e., the non-Abelian nature of the theory of strong interactions.

In Fig. 6 we also show the energy dependence of R_3 following from Abelian gauge theory (AGT; Ref. 77), which does not contain the gluon self-interaction and does not predict confinement. We see that AGT with rapidly growing coupling constant α_A completely disagrees with the experimental data.

4.5.2. Measurement of the coupling constant of the three-gluon vertex

An important feature of QCD as a non-Abelian gauge theory is the gluon self-interaction due to the fact that the gluon carries a color charge. This leads to the appearance of three-gluon vertices which, for example, must make a significant contribution to the production of four-jet events in e^+e^- annihilation, described by the graphs in Fig. 7. Although it is impossible to uniquely determine experimentally in which of these processes each individual four-jet event was formed, this can be done by statistical methods for a certain event sample after ordering of the jet energy in the form $E_1 \geq E_2 \geq E_3 \geq E_4$ on the basis of the specific structure of the jet from the three-gluon vertex.[78] One of the variables in which the distribution is different for the final states $q\bar{q}q\bar{q}$ and $q\bar{q}gg$ is the angle Θ^*_{NR} between $(\vec{p}_1-\vec{p}_2)$ and $(\vec{p}_3-\vec{p}_4)$ (the Nachtmann–Reuter angle; Ref. 79). It has been suggested that the angle α_{34} between the two jets with smallest energy be used to distinguish $q\bar{q}gg$ states produced as a result of double gluon bremsstrahlung (graphs a and b in Fig. 7) from the states produced in the process with a triple gluon vertex (graph d).[80]

In Fig. 8 we show the distribution in $\cos\Theta^*_{\text{NR}}$ obtained using the data from the L3 detector together with the perturbative QCD and AGT calculations.[77] The significant difference between the distributions of four-jet events in $\cos\Theta^*_{\text{NR}}$ predicted by these models is due to the fact that for $y_{\text{cut}}=0.01$ QCD gives only 4.7% four-jet final states $q\bar{q}q\bar{q}$,

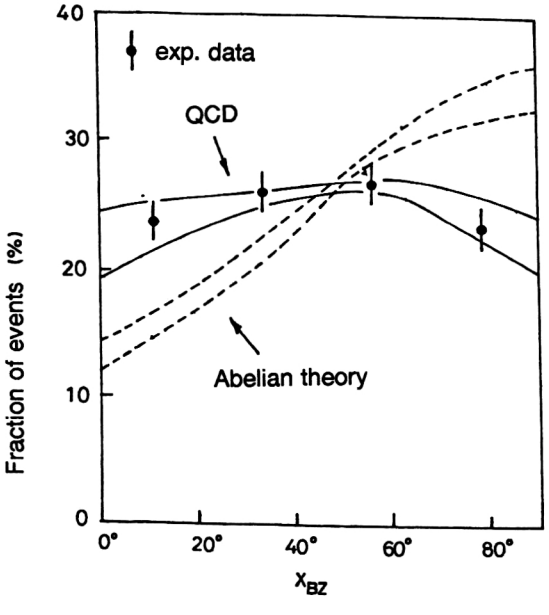

FIG. 8. Distribution of 4-jet events in $\cos\Theta^*_{\text{NR}}$ obtained at the L3 installation in e^+e^- annihilation at $\sqrt{s}=91$ GeV. The curves correspond to the results of calculations using QCD and the Abelian vector theory.

while AGT predicts 31.3% such states, because the graph with the three-gluon vertex does not exist in it.

The DELPHI Collaboration approximated the two-dimensional four-jet distribution in $\cos\Theta^*_{NR}$ vs. α_{34} by a dependence obtained in second-order perturbative QCD in which the ratios C_A/C_F and N_C/N_A (where C_A and C_F are the coupling constants at the ggg and qgq vertices, respectively, and N_C and N_A are the numbers of color charges of the quark and gluon) were taken as free parameters. In this study four-jet events were selected using the LUCLUS algorithm;[60] the background arising from falsely interpreted two- and three-pronged events was taken into account by MC modeling. A complicated analysis including all detector-related effects[81] gave $C_A/C_F=2.12\pm0.35$ and $N_C/N_A=0.46\pm0.19$, which are consistent with the corresponding values of 2.25 and 3/8 obtained in QCD.

The presence of a contribution from the three-gluon vertex was also established in analyzing the data of the ALEPH detector.[82]

4.6. Main characteristics of hadronic jets

Although e^+e^- annihilation presents ideal conditions for studying the structure of hadronic jets, owing to the features of gluon cascade development the determination of individual jets from quark fragmentation and, to an even greater extent, from gluon fragmentation at low energies is not completely unique. Therefore, up to LEP energies it is not the characteristics of individual jets that are usually studied, but those of annihilation events as a whole, assuming that two-jet events give the dominant contribution.

A detailed study of the structure of annihilation events in the range $\sqrt{s}=14$–34 GeV has been carried out at the TASSO setup.[83] The analysis of the energy dependence of the average charged-particle multiplicity that they performed, in which data at lower energies were also used, showed that it is described well by a dependence of the type $\langle n_{ch}\rangle=a+b\exp[c(\ln(s/Q_0^2))^{1/2}]$, with $Q_0=1$ GeV, obtained in the leading-log approximation of perturbative QCD. The values of $\langle n_{ch}\rangle/D$ (where D is the dispersion of the n_{ch} distribution) for charged particles emitted into opposite hemispheres relative to the sphericity axis which were found in Ref. 83 turned out to be about $\sqrt{2}$ times smaller than for the complete events, which indicates the absence of strong correlations between jets. The momentum distributions of the particles in the jet were analyzed assuming that the axes of the quark jets coincide with the thrust axis (see Sec. 4.1). It has been found that as $\sqrt{s}$ increases the number of particles emitted at small angles α to the jet axis grows rapidly, but for $\alpha>40°$ it is practically independent of the energy. The strengthening of the jet collimation with increasing jet energy is confirmed by the distributions of the normalized charged-particle momentum flux:

$$\frac{dP}{d\alpha}=\frac{1}{N}\int dp\,\frac{p}{\Sigma p_i}\,\frac{d^2N}{dpd\alpha},$$

which are shown in Fig. 9. It was found that the average transverse momentum of the charged particles relative to the jet axis depends nearly linearly on p_L for $p_L>0.5$ GeV/c.

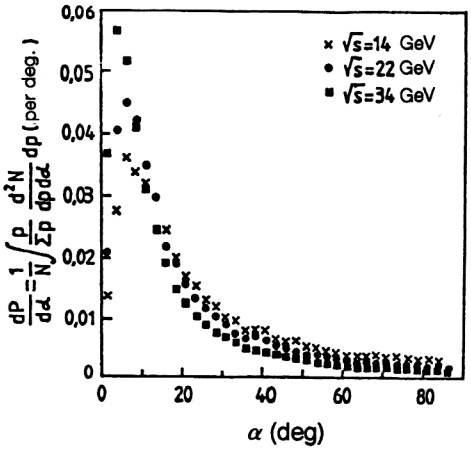

FIG. 9. Dependence of the charged hadron momentum flux on the angle α to the jet axis in two-jet events from e^+e^- annihilation.

However, the most impressive confirmation of the QCD predictions regarding parton fragmentation mechanisms was obtained in studying the distribution $(1/\sigma_t)(d\sigma/d\ln(1/x_p))$, where $x_p=2p/\sqrt{s}$, in which the "peaked plateau" predicted in Refs. 19 and 22 was found. This feature of the distribution in $\ln(1/x_p)$ was later confirmed at LEP energies using the OPAL detector.[84] In Fig. 10 we show the distribution in $\ln(1/x_p)$ obtained using this detector, together with the results of calculations using Eqs. (6) and (7). We see that the distribution deviates from a Gaussian, but the region of large x_p is described poorly by both equations. On the other hand, as shown in that study, the shape of this distribution completely reproduces the curve calculated using the HERWIG program. A joint analysis of the data obtained at the TASSO and OPAL detectors showed that the shift of the maximum with energy is consistent with the dependence following from Eq. (6), which confirms the presence of coherence effects in the development of the gluon cascade.

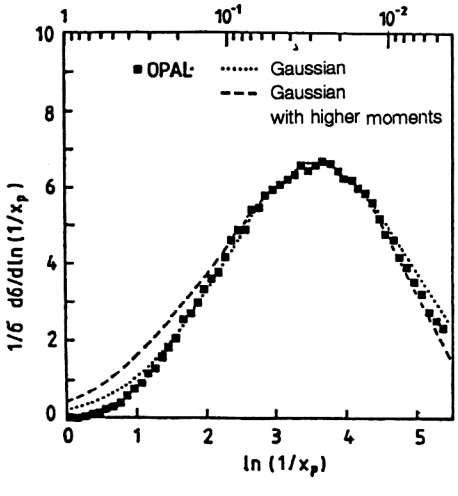

FIG. 10. Distribution in $\ln(1/x_p)$ of charged hadrons in e^+e^- annihilation at $\sqrt{s}=91$ GeV. The dashed line shows the result of calculations using Eq. (7) and the dotted line is the Gaussian distribution (6).

At present, studies of correlations between the kinematical variables of two and more hadrons belonging to the same jet are at a less advanced stage (from the viewpoint of both theory and experiment).

The positive short-range correlations between the rapidities of two hadrons with small $x_E = E_h/E_j$ predicted for the gluon cascade (see Sec. 2.3) were in principle discovered at the OPAL detector.[85] However, the experimental results differ considerably in details from the theoretical predictions made at a semiqualitative level.

In several experiments (see, for example, Ref. 86) strong negative short-range correlations between the charges of two hadrons have been found, indicating a local charge cancellation. On the other hand, the presence of a local cancellation of the transverse momentum has not been established.

4.7. Results of searches for differences in the structure of jets from gluon and quark fragmentation

As shown in Sec. 2.2, one of the most important predictions following from the QCD approach to strong interactions is the important difference between the quark and gluon hadronization processes owing to the larger color charge of the gluons. Therefore, right after the discovery of the gluon the structure of hadronic jets from gluon and quark fragmentation became the object of careful experimental study. Events of reaction (9), which possess the simplest parton structure, are usually used for this purpose. However, even in this case at the PETRA and PEP energies problems arose with the identification of jets from quarks and gluons, so different indirect methods of comparing them were used.

Although the studies carried out at these colliders gave conflicting results,[87–90] on the whole for $\sqrt{s} \leqslant 35$ GeV they indicated the absence of the significant difference between the gluon and quark fragmentation processes predicted by "naive" QCD.

This conclusion was confirmed in subsequent experiments carried out at higher energies. In the experiment carried out using TRISTAN at $\sqrt{s} = 50$ and 60.8 GeV (Ref. 91), the jet of lowest energy was selected as the gluon jet in 3-jet events, and the characteristics of the other jets (by assumption, produced by quarks) in 3-jet events were, as a control, compared to those of jets in 2-jet events selected in the same experiment. There was found to be a significant difference between the jets from quark and gluon fragmentation defined in this way in the dependence on the jet energy of the fraction of jet energy lying inside a narrow cone about the jet axis, the average rapidity of the leading particle in the jet, and the angular correlations. The difference that was observed qualitatively corresponded to the results of calculations using the JETSET program, in which the difference in the description of the quark and gluon fragmentation processes was taken into account.

The first attempt to make quantitative measurements of the difference in the structure of quark and gluon jets was made at the OPAL setup at $\sqrt{s} = M_{Z^0}$ (Ref. 92). The OPAL Collaboration recently published improved data on this question.[93] Roughly 23 thousand 3-jet events of reaction (9) were used in this experiment, which is more than an order of magnitude greater than the statistics used in the previous studies of this problem. The 3-jet events were selected using the k_t algorithm.

The large statistics made it possible to efficiently use the technique of quark jet tagging using the secondary vertex from the decay of c or b quarks. Here one of the quark jets was taken to be the fastest jet whose energy was at least 8 GeV higher than the energy of any of the slower jets. Then events were selected in which the remaining quark and gluon jets had similar energies (about 24 GeV), and the constraint $\psi_{qi} = (150° \pm 10°)$ was imposed on the angle ψ_{qi} between the axis of the fast-quark jet and the axis of the i jet. In addition, it was required that one of these jets contain a secondary vertex lying close to the e^+e^--interaction vertex. These criteria were used to select 1175 events with a tagged quark jet. By means of modeling it was found that the untagged slow jet was, with $(80 \pm 5\%)$ probability, a jet from gluon fragmentation. The 20% contamination of the sample by quark jets was corrected for in the rest of the analysis.

However, since the jet tagging process led to the selection of jets with heavy-quark production, the obtained distribution in the energy flux in the slow-quark jet must differ from the same distribution for random quark jets and it cannot be directly compared to such a distribution for gluon jets. Therefore, a second sample of 3-jet events with similar kinematical configuration but without tagged jets was used in this experiment. In this sample the set of slow jets appeared to be an equal mixture of gluon and quark jets, and the parameters of the slow-quark jet were obtained by subtracting the gluon jets from the first sample. In Fig. 11a we give the final distribution of the energy flux in the angle ψ_{qi} for jets from quark fragmentation obtained for the sample containing tagged jets, and in Fig. 11b we show the analogous distribution for jets from gluon fragmentation. The solid-line histograms in these figures show the results of modeling using the JETSET program. It follows from comparison of the distributions in Fig. 11 that the energy flux of the quark jet inside the jet "core" $(135° < \psi_{qi} < 165°)$ is considerably higher than in the gluon jet. In Fig. 12 we show the ratio of the normalized inclusive distributions $(1/n_{\text{tot}})(dn/dx_E)$ of particles from gluon and quark jets, where $x_E = E/E_j$. We see that soft particles dominate in a gluon jet. In this study it was reliably established for the first time that the average particle multiplicities in the range of jets $(120° < \psi_{qi} < 180°)$ from gluon and quark fragmentation differ considerably:

$$\frac{\langle n_{\text{tot}} \rangle_g}{\langle n_{\text{tot}} \rangle_q} = 1.267 \pm 0.043 \text{ stat.} \pm 0.055 \text{ sys.},$$

$$\frac{\langle n_{\text{ch}} \rangle_g}{\langle n_{\text{ch}} \rangle_q} = 1.326 \pm 0.054 \text{ stat.} \pm 0.073 \text{ sys.}$$

5. JET PRODUCTION IN HADRON–HADRON INTERACTIONS

Experiments to seek hadronic jets in hh interactions were begun at the same time as the analogous experiments in e^+e^- annihilation. However, the first reliable data on the observation of jets in pp interactions were obtained at the Intersecting Storage Rings (ISR) at CERN considerably later

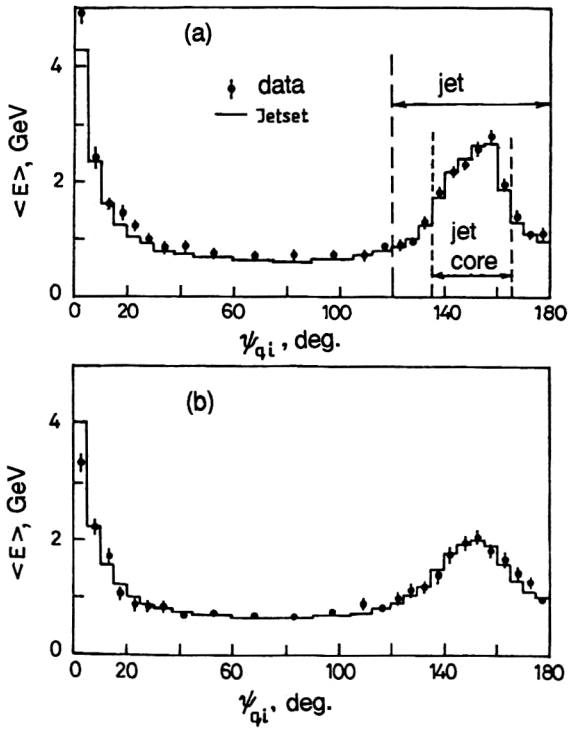

FIG. 11. Distribution of the energy flux as a function of the angle ψ_{qi} (see the text) for charged particles from three-prong events from e^+e^- annihilation at $\sqrt{s}=91$ GeV:
(a) For jets from quark fragmentation;
(b) For jets from gluons.

than at e^+e^- colliders. The delay was caused by the fact that the problem of distinguishing jets in hh interactions is more difficult experimentally than in e^+e^- annihilation owing to the presence of several quarks in the initial state. Up to now the main reaction used to study jets in hh interactions has been the hard scattering of two partons:

$$\begin{aligned} &h_1+h_2=q_1+q_2[+(n-2)q_{sp}]\to q_1+q_2+X_1 \\ &h_1+h_2=q+g[+(n-1)q_{sp}]\to q+g+X_2 \qquad (11) \\ &h_1+h_2=g_1+g_2[+(n)q_{sp}]\to g_1+g_2+X_3, \end{aligned}$$

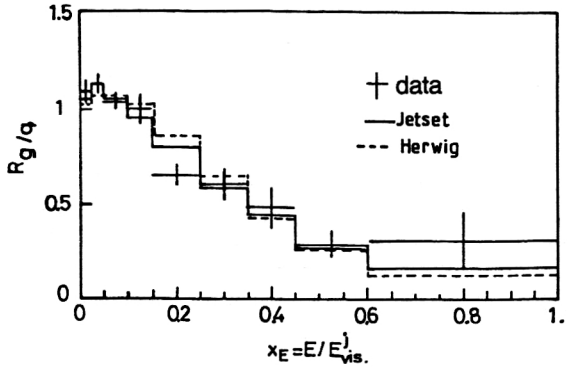

FIG. 12. Ratio $R_{g/q}$ of differential cross sections $(1/n_{tot})(dn/dx_E)$ for quark and gluon jets.

where n is the number of valence quarks in the colliding partons, leading to the appearance in the final state of two jets emitted at large angles to the primary hadron direction, and two beams of superimposed jets from the other spectator quarks q_{sp} emitted in the direction of the colliding beams, which in reaction (11) as written above are included in the system X_i.

At ISR energies the cross section for this process is small, so the main problem was to set up a trigger allowing the selection of events with two jets emitted at large angles in a background of soft interactions exceeding the effect of interest by several orders of magnitude. In addition, in contrast to e^+e^- annihilation, the jets produced in reaction (11) are not collinear in the c.m. frame of the colliding hadrons, since the interacting partons carry different fractions of the primary hadron momentum and have different values of the initial transverse momentum k_t. Moreover, along with the two jets from parton hard scattering in the final state of reaction (11), additional jets can appear from the gluons emitted by partons of the initial and final states, as shown in Secs. 2 and 3.

Hints of the possible existence of the process (11) were seen at the ISR even in the early 1970s, when it was discovered that the measured cross section for hadron production at large (≥ 1 GeV/c) transverse momenta significantly exceeds that expected on the basis of simple extrapolation of the data from the region of smaller $\sqrt{s}$(Ref. 2). The first convincing data on the production in pp interactions at the ISR of two hadronic jets from the fragmentation of partons produced in the reaction (11) were reported at the Twenty-First International Conference on High Energy Physics in 1982 (Ref. 94). It is interesting to note that at the same conference the UA2 Collaboration presented preliminary results on the discovery of jets at the CERN $\bar{p}p$ collider at $\sqrt{s}=540$ GeV, where this effect was much more pronounced.

5.1. Jet identification at ISR energies

The most detailed studies of reaction (11) at ISR energies were carried out using the Axial Field Spectrometer (AFS; Ref. 95), which already offered many of the possibilities of the experimental setups with 4π geometry later used at more powerful hadron colliders. In particular, the AFS had a precision sampling calorimeter with an absorber made of uranium and copper plates alternating with scintillating material, which covered the entire azimuthal angle φ in the rapidity range $|y|\leq 0.9$. This made it possible to accurately measure the total transverse energy ΣE_t and to set up a hard-interaction trigger using the calorimeter data.[96] In the AFS the regions of the calorimeter hit by particles from jets were distinguished using a LUCLUS-type algorithm.[60] Preliminary selection of two-jet events of reaction (11) was accomplished using the circularity C, a collective variable which is the two-dimensional equivalent of the sphericity S defined in Sec. 4.1.

It was shown that for $\Sigma E_t>25$ GeV, the event distribution in the circularity contains a peak at small values of C, which becomes dominant in distributions of events with $\Sigma E_t>35$ GeV. This feature of the distributions of the variable C in the range $30<\sqrt{s}<63$ GeV depends weakly on the

energy, but the number of events with large values of ΣE_t grows rapidly with increasing $\sqrt{s}$. It was also shown that two jets distinguished in events with $C<0.4$ by means of the cluster algorithm are emitted in opposite directions in the azimuthal angle φ [for $\Sigma E_t>44$ GeV, $\langle\Delta\varphi\rangle=(174\pm1)^0$], as should occur in the case of hard parton scattering. The measured cross sections of events with two jets in the range $\sqrt{s}=30-63$ GeV are also consistent with the results of calculations in lowest-order perturbative QCD.

In studying jet structure at the AFS setup it was established that the distribution of charged particles included in the jet in the quantity $x_p = 2p/\sqrt{s'}$, where s' is the energy of the colliding partons in the c.m. frame and for $\sqrt{s}=63$ GeV was $\langle\sqrt{s'}\rangle \simeq 32$ GeV for the selected events with $\Sigma E_t>33$ GeV and $C<0.4$, is in good agreement with the analogous distribution measured for two-jet events from e^+e^- annihilation at $\sqrt{s}=34$ GeV at the TASSO setup.[83]

To determine the nature of the partons producing jets with large p_t, the dependence of the ratio of the numbers of positive and negative particles in the jet as a function of their x_p was studied. The significant increase of this ratio with increasing x_p was interpreted as evidence that the fragmenting objects are mainly valence quarks which have undergone hard scattering.

Similar results were obtained at $\sqrt{s}=63$ GeV by the CMOR Collaboration[97] at a setup having an electromagnetic calorimeter covering 90% of the range of φ. In this experiment the trigger was set up using the total transverse energy ΣE_t^0 of the neutral particles (mainly π^0 mesons). The jet search algorithm was based on the assumption that the data from electromagnetic calorimeters contain only two clusters lying in the two different hemispheres. The jet size was then defined as the opening angle of the cone about the jet axis ($\theta_i<30°$). In this experiment, on the basis of the fact that the number of events in which both leading particles are positively charged increases with increasing ΣE_t^0, it was also concluded that the fragmenting partons are primarily u quarks.

5.2. Main results of jet studies at $\bar{p}p$ colliders

More detailed studies of hadroproduction of jets and their characteristics were carried out after the $\bar{p}p$ colliders at CERN and FNAL with energies of $\sqrt{s}=540-630$GeV and 800 GeV, respectively, came into operation. In this new energy range the cross sections for hard parton scattering processes rose sharply (for example, the cross section at $\sqrt{s}=540$ GeV turned out to be three orders of magnitude larger than at the maximum ISR energy), which ensured that they could be very clearly distinguished on the background of soft hadron interactions.

Hard processes at the CERN $\bar{p}p$ collider were mainly studied using two experimental setups, called UA1 and UA2 (from Underground Area) after the two underground areas in which they were located.

These two very different setups became famous because they were the ones to discover the vector gauge bosons $W^{\pm}$ and Z^0. But these setups also proved to be very effective tools for studying hadronic jets. Since in the hadronic jet studies carried out at them the jet identification algorithms differed considerably from the ones described above for e^+e^- colliders and took into account the special features of these detectors, here we shall describe their main characteristics.

The UA1 setup (Refs. 98–100) used a dipole electromagnet of the closed type with $H=0.7$ T, constructed initially for ISR experiments, in which the nearly hermetic yoke, interleaved with layers of plastic scintillator, served as a hadronic calorimeter (HC) covering the region $|\eta|<3$, where the pseudorapidity $\eta=-\ln[\tan(\Theta/2)]$. In the transverse direction the HC was segmented into 360 cells with independent information readout. Inside the yoke was a sampling (lead/scintillator) electromagnetic calorimeter (EMC) and a central cylindrical drift chamber 5.8 m long and 2.3 m in diameter. The calorimeters and track detectors were also used to cover small angles ($3\leq|\eta|\leq4$). The magnet was covered on the outside (except for its faces) by an additional 60 cm of iron filter and two layers of wire detectors for muon detection. This UA1 setup operated until the conclusion of research at the $\bar{p}p$ collider, and during that time only underwent some minor improvements (for example, the muon filter was enhanced).

In 1986 work began on replacing the EMC and enhancing the HC by placing inside the magnet a new combined (EMC+HC) calorimeter of the ionization type with uranium plates, in which the "warm" organic liquid tetramethylpentane (TMP) was used as the active medium. It was not possible to finish on time owing to problems with purifying the TMP, although interesting methodological results were obtained in this process.[101]

The UA2 detector, which was more modest in size and did not have a magnet, was successfully modernized in the mid-1980s and transformed into one of the most effective devices for studying hard processes. In the initial configuration, the main part of the UA2 detector was a set of central spherical sampling HCs (iron/scintillator) and EMCs (lead/scintillator) covering the region $|\eta|<1$ and hermetic in φ. These were broken up into 240 towers (cells) possessing projective geometry (i.e., "pointing" toward the center of the beam intersection region) and having transverse dimensions $\Delta\eta=0.1$ and $\Delta\varphi=15°$ (Ref. 102). A vertex detector 2 m long and 0.7 m in diameter made of cylindrical proportional and drift chambers was located inside the calorimeters (Ref. 103). Each end ($1<|\eta|<1.7$) was equipped with 12 small magnetic spectrometers made of toroidal magnets, wire chambers, and EMC blocks.[104,105] However, this exotic structure did not justify itself in actual operation, and the main results during the first phase of study at the CERN $\bar{p}p$ collider (1982–1985) using the UA2 setup were obtained using central calorimeters and a track system with acceptance in $|\eta|$ considerably smaller than that of UA1, so that larger statistics were required. Therefore, the first results on jet production processes are usually attributed to the UA1 Collaboration. In the course of modernization of the UA2 detector the end spectrometers were replaced by simple end calorimeters: EMCs (lead/scintillator) and HCs (iron/scintillator) covering the region $1\leq|\eta|\leq3$. The new central drift chamber of the "jet" type[106] was surrounded by two

cylindrical layers of silicon detectors with a pad structure.[107] The electron identification was improved by adding a cylindrical detector of transition radiation[108] and a preradiator with a coordinate detector composed of 60 thousand scintillating fibers 1 mm in diameter.[109]

These improvements during the final stage of investigations using the new Antiproton Collector (ACOL; 1988–1990) transformed UA2 into the main detector at the CERN $\bar{p}p$ collider, in spite of the fact that it did not contain a muon spectrometer.

The experience gained in using these detectors was put to use in the development of an experimental base for the FNAL $\bar{p}p$ collider, where two large calorimetric detectors were also developed.

The first of these is the Collider Detector at Fermilab (CDF; Ref. 110), which was put into operation in 1985.

The construction of this detector, which was the first of the second generation of collider detectors, represented a new stage in the development of techniques for research in colliding hadron beams at high energy. CDF is a classic detector with 4π geometry. Its calorimeters cover a pseudorapidity range of $|\eta|<4.2$ and are hermetic in φ. Inside the calorimeters are a central magnetic spectrometer, including a superconducting solenoid 5 m long and 1.5 m in radius transparent to radiation, which induces an axially symmetric magnetic field of strength $H=1.4T$, a central track system of 84 layers of cylindrical drift chambers, and a small vertex chamber of the time–projection type around the interaction region. This spectrometer ensures an accuracy of measuring the transverse momentum of a charged particle $p_t/p_t^2\approx 0.0015$ $(\mathrm{GeV}/c)^{-1}$ in the region $|\eta|\leqslant 1.2$. The central EMCs and HCs of the sampling type on the scintillator, which cover a range $|\eta|<1.1$, have transverse segmentation with projective geometry; $\Delta\eta\times\Delta\varphi=0.1\times 15^0$, and the face and side calorimeters on the proportional gas tubes have cells of dimension $\Delta\eta\times\Delta\varphi=0.1\times 5^0$. In the central part of the setup behind the HC is a layer of drift chambers of the muon system and the yoke of a magnet of thickness 60 cm. Muons at smaller angles are measured by muon spectrometers located behind the front calorimeters. Each of these spectrometers consists of two magnetized iron toroids about 7 m in diameter surrounded by drift chambers.

This detector may also become a part of the history of physics, since it may be used to discover the t quark in the near future.[111]

The second detector used since 1992 in the colliding beams of the $\bar{p}p$ collider is a large calorimetric spectrometer without a magnet, the DO, named for the beam intersection site at which it is located.[112] The distinctive feature of this detector is the liquid argon calorimeter with absorber of uranium and copper plates containing EMC and HC sections,[113] and its muon spectrometer, which is more powerful than that of CDF.

In all these setups the calorimeters play the fundamental role in studying jets, and one of the main methodological problems is that of reliably distinguishing the calorimeter cells struck by hadronic jets in the background of hadrons from the fragmentation of spectator quarks and bremsstrahlung gluons. Therefore, for analyzing the data here it was necessary to have more efficient algorithms for individual jet recognition based on the data on the jet structure obtained at e^+e^- colliders.

In the first stage of jet studies at the CERN $\bar{p}p$ collider the main problem was the verification of the fundamental ideas of QCD by comparing the experimental data with calculations carried out in lowest-order perturbative QCD. Such calculations for $2\to 2$ processes were carried out in $O(\alpha_s^2)$ already in the late 1970s (Refs. 115 and 116). The matrix elements for $2\to 3$ processes were calculated in the $O(\alpha_s^3)$ approximation in the early 1980s (Refs. 117 and 118):

$$\begin{aligned} &\bar{q}q\to\bar{q}qg \\ &q(\bar{q})g\to q(\bar{q})gg \\ &g_1g_2\to g_1g_2g_3, \end{aligned} \tag{12}$$

which had physical meaning only for certain configurations of three-parton states. Since at the time experiments at the CERN $\bar{p}p$ collider began the technique for perturbative QCD calculations allowing the inclusion of higher orders in α_s had not yet been developed for inclusive jet production, at that time no special requirements were imposed on the procedure for jet recognition in hh interactions like the requirements on the jet recognition algorithms in e^+e^- interactions discussed in Sec. 4.3. Therefore, several algorithms were developed for isolating individual jets with high energy taking into account the features of the detector.

For the UA1 detector, in which the magnetic field was perpendicular to the colliding beams, a cone-type algorithm was designed and used successfully.[119] It consists of the following sequence of operations:

- Each calorimeter cell is assigned an energy "vector," the absolute value of which is equal to the energy release in the cell, and the direction of which is the average direction from the interaction point to the centers of the energy release in the electromagnetic and hadronic parts of the calorimeter;
- All cells j with $E_t^j > E_t^{\mathrm{init}}$ (actually, $E_t^{\mathrm{init}} = 2.5$ GeV was used first, but then this threshold was lowered to 1.5 GeV) are assumed to be "initiating" cells and are arranged in order of decreasing E_t.
- The cell j_1 with the maximum E_t^j is taken to be the center of the first jet.
- The energies of all the initiating cells j located a distance $R = \sqrt{\Delta\varphi^2+\Delta\eta^2} < R_0$ from it, where $\Delta\varphi = \varphi_{j_1} - \varphi_j$ (φ is in radians) and $\Delta\eta = \eta_{j_1} - \eta_j$, are vectorially added to $\vec{E}_{t_1}$ (it was determined experimentally that $R_0=1$).
- The initiating cell with the maximum of the remaining E_t^j located outside this region is taken to be the center of the new jet.
- This procedure is repeated until all the initiating cells are included in one of the jets.
- At the conclusion of the procedure the energies of cells i with $E_t^i < E_t^{\mathrm{init}}$ are added to those jets relative to whose axes they have $p_t<1$ GeV/c and angle θ less than 45°.

The UA2 Collaboration has developed a cluster-type algorithm in which no *a priori* restrictions are imposed on the size and shape of the jet.[120]

The initial stages of operation of this algorithm, including the isolation of the initiating cells, were the same as for the UA1 algorithm described above. However, later all the adjacent cells (i.e., cells touching it on one side) with energy release $E_t^{\text{thr}} \geqslant 0.4$ GeV were added to the first initiating cell. To the adjacent cells in turn were added the cells adjacent to them with $E_t^{\text{thr}} > 0.4$ GeV, and this process was continued until no such cells remained. Assuming that such a cluster of cells with increased energy release corresponds to a jet absorbed in the calorimeter, its energy and direction were found by adding together the "vectors" $\vec{E}_t^j$ of all the cells included in the cluster. After this the new "embryo" of a jet was taken to be the one cell remaining outside the cluster of initiating cells whose E_t was a maximum, and the procedure was repeated. It turned out that jets with $E_t=2$ GeV selected in this manner occupy 3 cells on the average, while jets with $E_t=40$ GeV occupy about 10 cells. Clusters having a pair of local maxima separated by a "valley" of depth greater than 5 GeV were split into two. Although the UA2 algorithm we have described ensured good two-cluster resolution and has been used successfully for analyzing multicluster events, it underwent constant development as it was used. In particular, it was found that to take into account the parton energy loss due to gluon bremsstrahlung, it is necessary to add to the 3-momentum of a cluster with $E_t>10$ GeV the 3-momenta of all clusters with $E_t>3$ GeV which have small angles relative to the direction of the 3-momentum of this cluster ($\cos\omega > 0.2$). This procedure raised the E_t of the cluster by 15%.

The use of the jet recognition algorithms described above made it possible, even for the limited statistics obtained at the $\bar{p}p$ collider in the 1981–82 runs with integrated luminosity $\int L\,dt = 14\ \text{nb}^{-1}$, to obtain convincing proof of the existence in events with $\Sigma E_t \geqslant 40$ GeV of two hadronic jets emitted in opposite directions in azimuthal angle and possessing the dominant part of ΣE_t (Refs. 121 and 122).

The experience gained in jet recognition at the UA1 and UA2 setups was used in developing a jet search algorithm using the data from the CDF calorimeters. The CDF algorithm can be divided into the following three functional stages.[123]

A. Precluster creation

As in the UA1 algorithm, in the initial stage the initiating cells with energy release $E_t^j > E_t^{\text{thr}}$ are found and arranged in order of decreasing E_t^j (usually $E_t^{\text{thr}} = 1$ GeV is taken). During this procedure the cells in the end and side calorimeters are combined into groups of three in the coordinate φ so as to ensure that they have the same size as the cells of the central calorimeter. The preclusters were formed from a continuous chain of initiating cells falling in a "window" of 7×7 cells. The initiating cells falling outside the window were used as the start of the next precluster. The procedure was repeated until the full list of initiating cells was exhausted.

B. Cluster formation

Cells of natural size (i.e., without combining them in φ) were used again during the stage of cluster formation. For each precluster the coordinate of its center was calculated as the energy-weighted average of the coordinates of the centers of the cells included in it, and a circle of radius R was drawn around it. Then all the cells with energy release greater than 0.1 GeV falling inside this circle were included in the cluster, the coordinates of its center were recalculated, a new circle was drawn around it, and this iterative process was continued until complete convergence occurred.

C. Isolation of individual jets

Since part of the clusters created using the above procedure overlapped, i.e., the same cell could be included in two or more clusters, the CDF Collaboration formulated the following criteria for isolating individual jets. For two overlapping clusters the fraction of the energy of the smallest of the clusters located in the overlap region was determined. If this fraction turned out to be smaller than a given threshold (usually 75%), the overlapping clusters were split into two individual jets, and the cells in common were redistributed between the clusters according to the principle of smallest distance from the center of the jet. If the overlap turned out to be larger than the threshold value, the clusters were merged, which led to repetition of the iterative procedure for isolating a jet using all the cells. Finally, the transverse energy of the jet E_t^j was determined by summing over all the calorimeter cells assigned to the cluster, and the coordinates of the jet axis η and φ were calculated as the average of the corresponding coordinates of these cells weighted by E_t.

At the time the CDF experiments began, the first calculations of the cross section for the inclusive hadroproduction of jets using perturbative QCD including the next-to-leading order appeared.[125] In these calculations of the inclusive cross section using the three-parton matrix element it was necessary to introduce procedures for distinguishing a jet from two partons in the case of small spatial separation analogous to those used in the experiment. Since in the theoretical calculations it was natural to describe a jet in the form of a cone, it was necessary to find a definition for the size of this cone consistent with that of the experimentalists. In 1990 this problem became the subject of special discussion at the Summer School on High Energy Physics at Snowmass (USA). As a result, it was agreed that in studying inclusive jet production at the energies of existing $\bar{p}p$ colliders the standard would be the definition of a jet as a cone with $R=0.7$ in the variables $\eta-\varphi$. This definition was suitable for the FNAL energy both from the viewpoint of the magnitude of the background from hadrons not belonging to the jet but falling inside the cone, and from the viewpoint of the loss of fragmentation particles falling outside the cone. However, the main argument in favor of this jet definition was that in perturbative QCD calculations in $O(\alpha_s^3)$ for this cone size the dependence of the calculated results on the renormalization scale parameter μ is minimal.

5.2.1. Cross sections for inclusive jet production

The features of inclusive jet production in the reaction

$$\bar{p}p \to j + X \tag{13}$$

have been studied by the UA1 and UA2 Collaborations over several years with gradually increasing integrated luminosity (Refs. 122, 124, and 127). Measurements of the differential cross sections for inclusive jet production $d\sigma/dE_t^j d\eta$ have been made up to $E_t^j \sim 150$ GeV using the experimental data

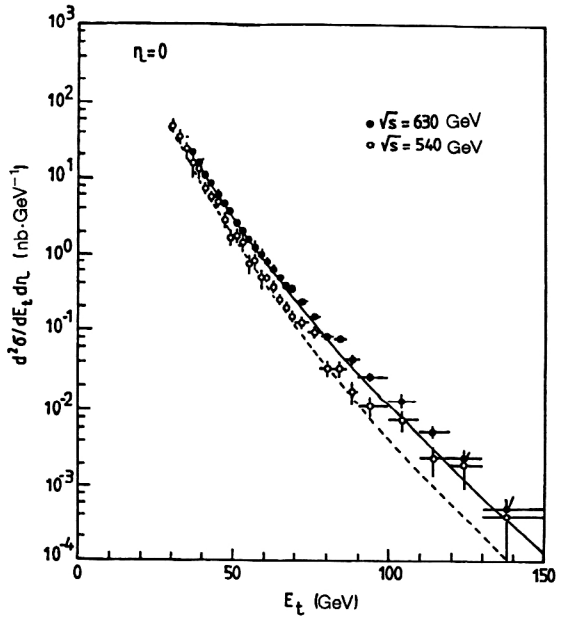

FIG. 13. Inclusive distribution $d\sigma/dE_t$ of jets at $\sqrt{s}=540$ and 630 GeV. The dashed and solid lines show the results of the calculations in lowest-order perturbative QCD for these energies.

obtained at $\sqrt{s}=540$ GeV in the 1983 run with integrated luminosity ~ 120 nb^{-1} and for $\sqrt{s}=630$ GeV in the 1984 run with integrated luminosity ~ 310 nb^{-1}. The statistics in these runs were collected either using a trigger based on increased total transverse energy, $\Sigma E_t > 40$–60 GeV, or a trigger based on an increase in the local energy release in a limited region of the calorimeter. The systematic error in the measurement of the absolute cross section of reaction (13) at the UA1 and UA2 detectors was about 50%. The main source of systematic error was the large ($\sim 35\%$) uncertainty in the model-dependent calculations of the acceptance of the detector for one and two jets. The systematic error arising from the uncertainty in the calibration of the energy scale of the calorimeters was $\pm 20\%$, and the integrated luminosity at the beam intersection points was measured with about the same accuracy.[122]

Since some of these uncertainties disappear when comparing measurements made at a single detector, at the UA2 setup it proved possible to successfully determine the energy dependence of the cross section $d\sigma/dE_t^j d\eta$ from the measurements made at $\sqrt{s}=540$ and 630 GeV (Ref. 128). The results of these measurements, shown in Fig. 13, indicate a significant (by a factor of two) rise of the cross section for inclusive production of jets with $E_t^j > 60$ GeV in this region of $\sqrt{s}$.

The approximation of these cross sections by the standard expression for hard parton scattering,

$$Ed\sigma/dp^3 = p_t^{-n} f(x_t), \quad f(x_t) = A(1-x_t)^m/x_t^2. \qquad (14)$$

where $x_t = 2p_t/\sqrt{s}$, gave the parameter estimates $n = 4.5 \pm 0.3$ and $m = 7.3 \pm 0.2$.

The results of the perturbative QCD calculations shown in Fig. 13 qualitatively agree with the experimental data.

The final analysis of inclusive jet production at $\sqrt{s}=630$ GeV (Ref. 129) was carried out by the UA2 Collaboration for statistics of 7.5 pb^{-1}, obtained in 1988–89 using the modernized setup, which made it possible to extend the acceptance in the pseudorapidity to $|\eta| \leqslant 2$. The absolute accuracy of measuring the jet production cross section was raised to 32%. The use of Eq. (14) to approximate these new experimental data on $Ed\sigma/dp^3$ together with the data on the inclusive jet cross section at ISR energies and the preliminary data obtained at CDF for $\sqrt{s}=1800$ GeV gave improved estimates of the parameters: $n = 4.92 \pm 0.11$ and $m = 6.04 \pm 0.28$.

A quantitative test of the QCD predictions for hadroproduction of jets in a range of E_t^j broader than at the CERN $\bar{p}p$ collider has been performed at the CDF setup. The successful operation of the $\bar{p}p$ collider at FNAL made it possible for CDF to collect statistics of 45 pb^{-1} during the 1988–89 run. These data were obtained with a trigger to select events having a cluster with transverse energy greater than E_t^0 in the calorimeters. In order to increase the statistics for jets with large E_t, three values of the transverse energy (20, 40, and 60 GeV) were used in the trigger.

The cross section for inclusive jet production was measured at CDF in the range $E_t^j = 35$–450 GeV, where its value falls by seven orders of magnitude. The accurate calibration of the calorimeters by simultaneous measurement of the charged-hadron momenta in the central magnetic spectrometer of the CDF and detailed modeling of the influence of the limited energy resolution in E_t^j on the shape of $d\sigma_j/dE_t^j$ made it possible to decrease the systematic error in measuring the cross section for $E_t^j > 80$ GeV to 22% (Ref. 130). Together with the 10% increase of the accuracy of the perturbative QCD calculations owing to the inclusion of the order-α_s^3 term, this made it possible to perform for the first time a detailed study of the suitability of the different parametrizations of the parton structure functions in the nucleon for describing the hard scattering of partons of very high energy. In particular, it was found that form B of the structure-function parametrization in Ref. 131 [version HMRC(B)] is in good agreement with the experimental data over ten orders of magnitude variation of the cross sections.

One of the main goals of Ref. 130 was to check the composite-quark hypothesis.[132] The existence of unknown superstrong interactions binding the elementary constituents inside the quark should lead to a finite value of the constant Λ_c in the approximation of $d\sigma/dE_t$ by the theoretical dependence obtained in Ref. 132 for "extended" QCD incorporating this effect. An infinitely large value of Λ_c would correspond to "pure" QCD. In Ref. 130 it was found that at the 95% confidence level $\Lambda_c \geqslant 845$ GeV, i.e., quarks can be assumed to be noncomposite objects down to 1.4×10^{-4} F.

The CDF Collaboration has also studied the problem of violation of x_t scaling predicted by QCD in inclusive jet production in the range $\sqrt{s}=546$–1800 GeV. In Fig. 14 we show the x_t dependence obtained in Ref. 133 of the ratio of the corresponding inclusive cross sections, made dimensionless by multiplying by E_t^3, together with the $O(\alpha_s^3)$ QCD calculations with the structure functions in the HMRC(B) parametrization (Ref. 131). We see that for $x_t < 0.17$ the ex-

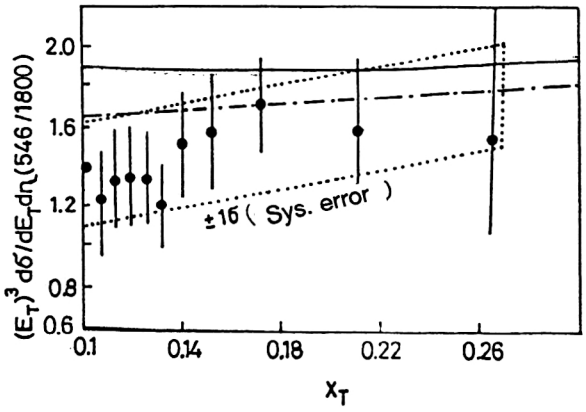

FIG. 14. Ratio of the cross sections $(E_t)^3 d\sigma/dE_t d\eta$ at $\sqrt{s}=546$ and 1800 GeV. The solid line is the result of perturbative QCD calculations including the $O(\alpha_s^3)$ term with the structure function in the HMRS(B) parametrization, $\mu=E_t/4$, and including jet superposition. The dot-dashed line is the same with correction of the jet energies for background hadrons.

perimental data not only demonstrate the absence of pure x_t scaling, but they differ considerably (by more than two standard deviations) from the QCD predictions. It should be noted that the disagreement of the experimental cross sections $d\sigma_j/dE_T$ at each of these energies with the calculations of $O(\alpha_s^2)$ perturbative QCD are not as important when ratios of them are considered owing to the large systematic errors, which partially cancel out. Additional studies have shown that this discrepancy cannot be eliminated by choice of the parton structure functions, but it can be decreased if the calculations more fully take into account the corrections for jet contamination by background hadrons for the jets isolated experimentally using the CDF algorithm.

5.2.2. Main characteristics of jet pair production

Studies of the inclusive process

$$\bar{p}p \rightarrow j_1 + j_2 + X, \tag{15}$$

performed using the data obtained at the CERN $\bar{p}p$ collider in the 1982 and 1983 runs by the UA1 and UA2 collaborations confirmed the earlier observation[122] that events with $\Sigma E_t > 40$ GeV have two clearly expressed leading jets in the central region which carry most of the transverse energy.

The appearance of two leading jets with large E_t can only be due to hard scattering processes (11) with the subsequent fragmentation of two partons,[134] so the effective detection of two-jet events at the UA1 and UA2 setups revealed the possibility of studying subprocesses (11) in a new energy range. However, it was necessary to introduce a number of important corrections to the experimental results in order to evaluate the parameters of the scattered partons sufficiently accurately on the basis of the kinematical characteristics of the jets measured by the calorimetric method. Among these corrections are ones for the losses arising in isolating the jet using the algorithms described above from the fraction of jet particles emitted at large angles to the jet axis; there are also energy-dependent corrections taking into account the nonlinearity of the calorimeter, leakage of part of the cascade from it, edge effects, and the presence of a dead zone (due to the mountings, the cable routings, the light guides, and so on). These corrections to the energy measured by the UA1 calorimeters were ~10% for hard jets. In addition, corrections were introduced for bremsstrahlung gluon emission by final-state partons (~12%) and a number of smaller corrections. As a result, the average energy resolution in the jet measurements in UA1 was $\delta E/E \simeq \pm 26\%$. Modeling showed that for UA1 the experimentally measured direction of the jet 3-momentum coincides with the direction of the vector sum of the momenta of particles from parton fragmentation with accuracy $\sigma_\varphi = 6°$ and $\sigma_\eta = 0.04$ (Ref. 135).

An example of the analysis of two-jet events is that of Ref. 136, performed for the UA1 data, in which the usual formalism of quasi-two-particle parton scattering was used. The differential cross section for the subprocesses (11) as a function of the scattering angle θ in the c.m. frame was written as

$$\frac{x_1 x_2 d^3\sigma}{dx_1 dx_2 d\cos\theta} = F_i(x_1)\cdot F_j(x_2) d\sigma_{ij}/d\cos\theta \tag{16}$$

where $F_i(x_1)$ and $F_j(x_2)$ are structure functions representing the density of the corresponding partons in the hadrons as a function of the relative longitudinal momenta x_1 and x_2 of these partons, and σ_{ij} is the cross section for quasielastic scattering, which corresponds to the calculations of lowest-order perturbative QCD. Since in QCD all processes occur via vector gluon exchange, they all have a complicated angular dependence, which for $\cos\theta \rightarrow 1$ tends to $(1-\cos\theta)^{-2}$. Assuming that two-jet production is dominated by quasielastic processes having identical angular dependence, the cross section for this process can be represented as (16), where the $F(x)$ become the effective structure functions for several types of parton. In particular, if $d\sigma/d\cos\theta$ is taken as the differential cross section of gluon–gluon scattering

$$d\sigma/d\cos\theta = 9/8(\pi\alpha_s^2/2x_1x_2s)(3+\cos^2\theta)^3(1-\cos^2\theta)^{-2}, \tag{17}$$

where s is the square of the total energy in the c.m. frame, then $F(x)$ can be written as

$$F(x) = G(x) + 4/9[Q(x) + \bar{Q}(x)], \tag{18}$$

where $G(x)$, $Q(x)$, and $\bar{Q}(x)$ are respectively the structure functions of the gluon, the quark, and the antiquark.

The distribution in $\cos\theta$ obtained in Ref. 136 is in good qualitative agreement with the results of the perturbative QCD calculations carried out in $O(\alpha_s^2)$, but in complete disagreement with the form of the angular dependence following from the Abelian theory with scalar gluons.[137] The approximation of the data in the region $|\cos\theta| > 0.4$ by a dependence $\sim(1-\cos\theta)^{-n}$ gave $n = 2.38 \pm 0.10$. In determining the structure functions $F(x)$ it is important to bear in mind the fact that the actual cross section for two-jet production must receive a contribution not only from Eq. (16), but also from higher orders of perturbative QCD. At the time the study of two-jet events was being performed by the UA1 collaboration there were no accurate calculations of these

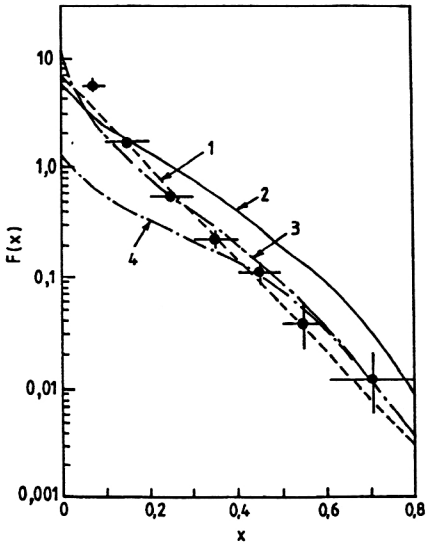

FIG. 15. Structure function $F(x)$ reconstructed from the UA1 data. Dashed line 1 is the result of approximation by an exponential; curve 2 is $F(x)$ for $Q^2=20$ GeV^2 with the parametrization of the CDHS experiment; curve 3 is the same structure function recalculated for $Q^2=2000$ GeV^2; curve 4 is the structure function for quarks $(4/9)(Q(x)+\bar{Q}(x))$.

corrections, and a multiplicative factor K was introduced for including them; according to several estimates, $K\approx 2$ (Ref. 138).

The structure function $F(x)$ shown in Fig. 15 was obtained in Ref. 136 assuming the factorization of the cross section in x_1 and x_2. In calculating this function it was assumed that $Q^2=-\hat{t}$, where $\hat{t}=(p_1-p_3)^2$ is the squared difference of the 4-vectors for the primary parton and the final-state parton having the largest energy. In the range $0.1<x<0.8$ this function was described well by an exponential dependence $F(x)=6.2\exp(-9.5x)$ (dashed line in Fig. 15). For comparison with the structure function $F(x)$ obtained in the UA1 experiment, in Fig. 15 we show the structure function (18) for $Q^2=20$ GeV, based on the parametrization of the CDHS experiment,[139] and the same function calculated for $Q^2\approx 2000$ GeV, which corresponds to $\langle Q^2\rangle$ for the UA1 experiment. The curve shows the structure function calculated only for the quark and antiquark. It follows from these distributions that the UA1 data indicate the presence in the proton of a high density of the gluon component at small x and demonstrate scaling violation at large Q^2.

These conclusions were later confirmed by studies carried out by the UA2 Collaboration[140] using data obtained in the 1983 run.

Studies of two-jet events for the purpose of determining the nucleon structure function have been carried out at the energy $\sqrt{s}=1800$GeV at the CDF setup using a much larger amount of data.

Because the experimental data on this process were compared to the results of the $O(\alpha_s^2)$ perturbative QCD calculations existing at that time, the cone size was chosen from the requirement of obtaining the best agreement with the experimental data. It was found from analysis of the data on the two-jet invariant-mass distribution $M(2j)$ that most parametrizations of the structure functions give a better description of the distribution $d\sigma/dM(2j)$ obtained when jets with $R=0.1$ are selected (Ref. 141). Therefore, a cone with $R=1.0$ was used for describing jets in all the CDF studies in which the experimental results were compared to the $O(\alpha_s^2)$ perturbative QCD calculations. In order to decrease the effect of processes of higher order in α_s, using the imbalance of $\vec{p}_t$ of the two leading jets as the basis, the smearing of the distributions in various variables owing to gluon bremsstrahlung was calculated (the E_t smearing function had the form of a Gaussian with width depending on E_t^j), and the results of the $O(\alpha_s^2)$ perturbative QCD calculations were modified using these functions. This technique was used in particular for analyzing the differential cross sections for two-jet production $d^3\sigma/dE_t d\eta_1 d\eta_2$ obtained by the CDF Collaboration in Ref. 142. In that study one jet lying in the region $|\eta_1|\leq 0.6$ had to have energy not less than E_t^{thr}, and the second leading jet with $E_t^j>2$ GeV could lie in the pseudorapidity range $|\eta_2|<2.8$. The differential cross sections in η_2 averaged over the range $|\eta_1|\leq 0.6$ for six ranges of E_t from 45 GeV to 225 GeV turned out to be especially critical for checking the structure functions in the range $0.04\leq x\leq 0.3$, where the gluon component plays the dominant role. The results of QCD calculations using 12 different forms of structure function giving 36 combinations were fitted to these experimental data by the least-squares method; some of these combinations proved to be inapplicable for describing the experimental distributions according to the χ^2 criterion.

5.2.3. Results of studies of multijet final states

Already for the first sets of events with high-energy hadronic jets obtained at the UA1 and UA2 setups it was found that, in addition to the two leading jets, 10–15% of the events have additional jets with $E_t^j>15$ GeV (Ref. 127). The presence of such jets was attributed to gluon bremsstrahlung by partons of the initial or final state.[143] However, the reliable separation of final states with three and more jets became possible only after the data processing techniques for these detectors had become well developed and sufficient data had been obtained.

Detailed studies of three-jet events have been carried out at the UA2 setup at $sqrts=630$ GeV (Ref. 120). In isolating three-jet events on the basis of the information obtained from the central calorimeters of the UA2 setup it was assumed that the two leading jets from fragmentation of the scattered partons are oriented in opposite directions in azimuthal angle, and that jets from bremsstrahlung gluon fragmentation must have lower energy and can be located near one of the leading jets. Therefore, to improve the two-cluster resolution a second phase was added to the cluster-search algorithm described above. This phase consisted of repeating the jet identification procedure another time using as the initial approximation the jet 3-momenta found in the first phase. However, here the threshold value was taken to be $E_t^{\text{thr}j}=0.05E_t^j$, which for high-energy jets was considerably greater than the initial choice $E_t^{\text{thr}}=0.4$ GeV. The cells of the initial clusters whose energies were smaller than the new value E_t^{thr} were redistributed in the second phase between the nearest new clusters. Methodical investigation showed that

by using the improved algorithm it was possible to isolate more than 80% of the jets for which the angle between their axes was $\omega \geqslant 40°$. After completion of the cluster selection they were ordered in E_t^j (the cluster with smallest E_t^j was taken first, and so on). Three-jet events were selected using the following criteria: $E_t^1+E_t^2+E_t^3>70$ GeV; $E_t^3>10$ GeV, $E_t^4<10$ GeV; $|\eta_i|<0.8$; $i=3$. To further clean the data of events with more than three jets the condition $\Sigma\vec{p}_t^{\,i}<20$ GeV was imposed so that the 3-momenta of the three jets would fairly accurately cancel each other out in the transverse plane. In this way practically exclusive sets of 3-jet events were obtained.

The final analysis of 3-jet events was carried out in the rest frame of the three jets, in which their positions can be described by six variables, for example, the three angles specifying the spatial location of the plane in which the 3-momenta of the three jets lie and the angles determining the configuration of the 3-jet system in this plane.

The first two angles are usually taken to be the polar and azimuthal angles θ^* and ϕ^{ast} between the 3-momentum of the jet with maximum energy, $\vec{p}_1^{\,*}$, and the direction of the primary beam. These are calculated using the rules formulated in Ref. 144. The additional angle characterizing the orientation of the two other jets is usually taken to be the angle ψ^* between the plane containing their 3-momenta and the plane containing $\vec{p}_1^{\,*}$ and the beam 3-momentum

$$\cos\psi^*=(\vec{p}_b\times\vec{p}_1^{\,*})(\vec{p}_2^{\,*}\times\vec{p}_3^{\,*})/[|\vec{p}_b\times\vec{p}_1^{\,*}|\times|\vec{p}_2^{\,*}\times\vec{p}_3^{\,*}|].$$

It was found that the distribution in $\cos\theta^*$ is in good agreement with the $O(\alpha_s^3)$ perturbative QCD calculations and with the analogous distribution obtained by analyzing two-jet events.[140] The distribution in ψ^* also agreed with the QCD calculations carried out for unpolarized beams. Study of the internal structure of the 3-jet system gave convincing evidence in favor of the existence of gluon bremsstrahlung processes.[144]

Similar agreement with the structure of the three-jet system predicted by QCD and the good QCD description of two-jet processes obtained earlier in the UA1 and UA2 experiments made it possible to measure the constant α_s on the basis of the ratio $R=\sigma(3j)/\sigma(2j)$. This was done by selecting the value of α_s that would make the ratio $R_{\rm QCD}$, calculated by the Monte Carlo method in QCD taking into account the features of jet identification in the UA2 detector and the technique of three-jet selection, equal to the ratio measured experimentally. The additional constraints described in Ref. 120 were imposed to make it easier to compare these ratios for sets of 2- and 3-jet events. The resulting experimental value was

$$R_{\rm exp}=0.177\pm0.04.$$

However, when this experiment was carried out the two- and three-jet cross sections had been calculated only in lowest-order perturbative QCD, and the K factor was introduced to take into account the higher-order terms contributing to these cross sections. Therefore, only an estimate was actually obtained in this experiment:

$$\alpha_s\times K_3/K_2=0.23\pm0.01\pm0.04,$$

where the second error is the systematic experimental error. In these calculations the square of the maximum transverse momentum of one of the jets, $Q^2=[\max(p_t^j)]^2$, was taken as the variable Q^2. This estimate agrees well in magnitude with the result obtained earlier by the UA1 Collaboration.[145] However, extrapolation of the estimate of α_s obtained earlier in e^+e^--annihilation experiments for $\sqrt{s}<35$ GeV (Ref. 146) to the average energy of collider experiments $\sqrt{s}\approx90$ GeV gave a result ~30% smaller than the one quoted above. This might arise both from K_3/K_2 being different from unity, and from uncertainty in the choice of the variable Q^2 for two- and three-jet events.[145]

The UA2 collaboration also analyzed the structure of multijet events for $\sqrt{s}=630$ GeV with ΣE_t in the range 15–210 GeV in terms of collective variables.[147] This analysis again made use of information from the central calorimeters, which recorded secondary hadrons only in a restricted part of the central region ($|\eta|\leqslant1$). The Fox–Wolfram moments[44] described in Sec. 4.1 were used to isolate sets of events with two and three jets without imposing any kinematical constraints on E_t of the jet. It was found that events with sufficiently large H_2 or H_3 (for example, $H_2>0.7$ and $H_3>0.22$) respectively have a clearly expressed two- and three-jet configuration, and the ratio of the numbers of them for $\Sigma E_t>100$ GeV is $R=N_3/N_2\simeq0.2$, which coincides with the above-described results of the study performed by the UA2 Collaboration, who used a different method. The polar graph of the transverse-energy flux in three-jet events was in good agreement with the graph of three-jet events in e^+e^- annihilation.

Events with $\Sigma E_t\geqslant120$ GeV having no less than three jets with $E_t^j>15$ GeV and with 3-momenta lying in the region $|\eta|<3.5$ and separated by $\Delta R>0.85$ in the $\eta-\varphi$ plane were selected in Ref. 150 for studying 3-jet events at $\sqrt{s}=1800$ GeV at CDF. About 4800 events remained for the final analysis after this selection. These states were analyzed as earlier in Ref. 120 in the rest frame of the three jets having the largest E_t^j. Since owing to the difference between the quark and gluon spins and the coupling constants at the qg and gg vertices the QCD predictions differ for different types of interacting parton, the distributions obtained at CDF in the angles θ^* and ψ^* defined above and in $x_i=2E_{ti}^j/M(3j)$ were used to find the contribution of various initial partons to $2\to3$ processes. For this the contributions of the six individual subprocesses of the $2\to3$ type with cross sections obtained using the parametrization of the parton structure functions of Ref. 148 were calculated separately. The matrix element for the $2\to3$ subprocess calculated in perturbative QCD for graphs without virtual corrections[149] were used in these calculations. In addition, the contribution of the initial $q\bar{q}$ state, $\alpha_{q\bar{q}}$, was taken as a separate parameter and independently determined by fitting the distributions from all processes (with fixed contributions aside from the process $q\bar{q}\to qqg$) to the experimental data. The resulting estimate $\alpha_{q\bar{q}}=0.03^{+0.04}_{-0.03}$ confirmed the predictions that $\sqrt{s}=1800$ GeV dominates hard gluon scattering. For example, in Fig. 16 we show the experimental distribution in the angle ψ^* together with the results of the calculation using "complete" QCD (i.e., including all $2\to3$ subprocesses) and for the sub-

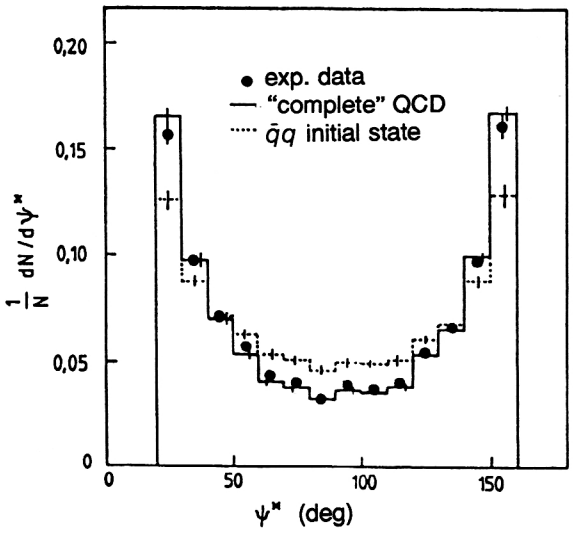

FIG. 16. Distribution in the angle ψ^* of three-jet events from $p\bar{p}$ interactions at $\sqrt{s}=1.8$ TeV.

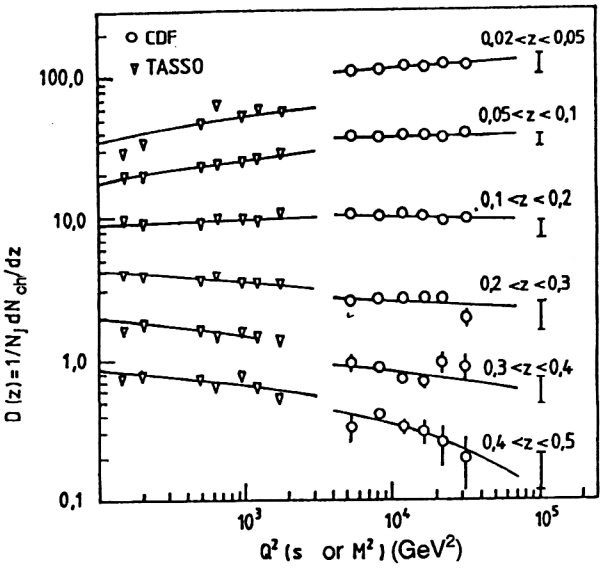

FIG. 17. Q^2 dependence of the fragmentation function $D(z)$ of jets from $\bar{p}p$ interactions at $\sqrt{s}=1.8$ TeV. The results of the measurements are shown only with their statistical errors. The systematic errors of the measurements are shown on the right. For comparison, in the same figure we show the analogous distributions measured at smaller Q^2 in e^+e^- annihilation.

process $\bar{q}q\to q\bar{q}g$. We see that the accuracy attained at CDF unambiguously indicates that the contribution of the latter subprocess is small.[130]

The data on events with ≥ 4 jets in $\bar{p}p$ interactions at the energies of the CERN and FNAL colliders are so far very limited owing to technical problems in isolating such events. An attempt was made at the UA2 setup at $\sqrt{s}=630$ GeV to measure the cross sections for events in which four, five, and six jets with energy $E_t^j>15$ GeV were produced at $|\eta_j|<2.0$. Altogether, 9947 four-jet events, 281 five-jet events, and 7 six-jet events were isolated, which with ~60% uncertainty gave cross sections $\sigma_{4j}\simeq 1.31$ nb, $\sigma_{5j}\simeq 0.037$ nb, and $\sigma_{6j}\simeq 0.009$ nb (Ref. 151). Since these cross sections coincided with the estimates obtained using higher orders of perturbative QCD, it was concluded in that study that double hard parton scattering is absent.

5.2.4. The structure of hadronic events at large E_t^j

The possibility of fairly cleanly isolating individual hadronic jets with $E_t>20$ GeV in experiments at $\bar{p}p$ colliders made it possible to study the structure of these events and compare the distribution of secondary particles inside high-energy jets with the analogous distributions obtained at e^+e^- colliders. Since at the energies of the CERN and FNAL $\bar{p}p$ colliders partons undergoing hard scattering must represent a mixture of quarks and gluons, while at large angles gluons should dominate over quarks,[122] such a comparison is important for checking the differences predicted by QCD between the gluon and quark fragmentation processes.[152] It was found that as E_t^j grows the halfwidth of the transverse-energy flux at half-max drops significantly; i.e., the jets become more collimated. On the other hand, study of the distribution of the charged-particle multiplicity flux inside the jet did not reveal any clear maximum at the center, i.e., in the jet core there is a limited number of leading hadrons carrying most of the E_t^j, and they become more important as E_t^j grows.

The fragmentation function $D(z)=1/N_c\cdot dN_{ch}/dz$ in the range $0.02<z<0.6$ reconstructed in Ref. 154 is on the whole in good agreement with the analogous distribution obtained in e^+e^- annihilation at $\sqrt{s}=34$ GeV (Ref. 83). On the basis of this it was concluded in Ref. 136 that the gluon and quark fragmentation functions do not markedly differ.

The multiplicity distributions of charged particles in a jet and the energy flux distribution inside a jet were studied in more detail somewhat later by the UA2 Collaboration for $\sim 3\times 10^4$ jets.[155] Comparison of the dependence of n_{ch}^j on $M(2j)$ that was found with the e^+e^--annihilation data at lower values of the c.m. energy and the parton-model calculations based on QCD[156] showed that the data on the $\langle n_{ch}^j\rangle$ dependence on $M(2j)$ in jets recorded in $\bar{p}p$ interactions at $\sqrt{s}=540$ GeV are closer to the theoretical predictions for gluon jets. The distributions of the transverse energy flux in $\Delta\varphi$ obtained for various ranges of E_t^j lay between the theoretical curves for gluon and quark jets and were considerably broader than the distributions obtained using the FFM with $q_t=350$ MeV/c.

Measurements of the fragmentation function of high-energy jets and its dependence on the two-jet invariant mass $M(2j)$ were continued at CDF. In Ref. 158 the fragmentation function was studied for statistics corresponding to integrated luminosity ~26 nb^{-1}. Events with two leading jets in the range $|\eta|<0.8$ and pointing in opposite directions in azimuthal angle ($\Delta\varphi=180°\pm 30°$) in which there was no third jet with $E_t^j>20$ GeV were selected for these studies. The value $R=1.0$ was used for jet selection. The z distribution of the charged particles obtained after these corrections was corrected for smearing effects related to the limited resolution of the magnetic spectrometer.

In Fig. 17 we show the distributions $D(z,Q^2)$ for various ranges of z as a function of the squared invariant mass

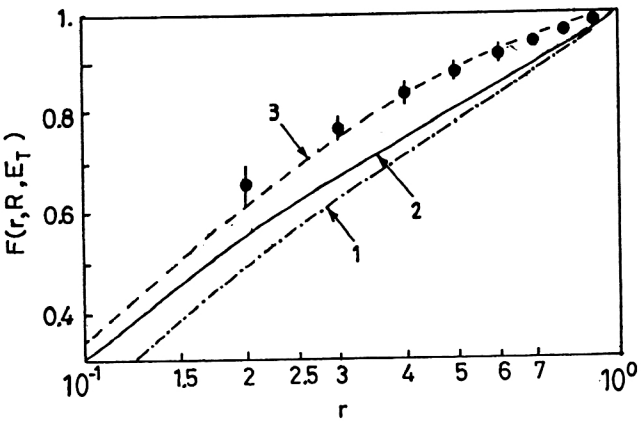

FIG. 18. Distribution in r of the function $F(r,R=1, E_t=100$ GeV) for jets identified at the CDF setup. Curve 1 is the result of perturbative QCD calculations including the α_s^3 term and $\mu=E_t/4$; curve 2 is the same with $\mu=E_t/2$; curve 3 is the same as curve 1, but with an improved procedure for the merging of close-lying jets.

$M^2(2j)$, which was taken as an estimate of Q^2. For comparison, in the same figure we give the s dependence of the fragmentation function obtained in e^+e^- annihilation at the TASSO setup.[83] We see that the two experiments display the same trend, indicating an increase in the number of particles with small z occurring with increasing Q^2, which is in qualitative agreement with the QCD evolution of $D(z,Q^2)$ (see, for example, Ref. 158).

Theory predicts that for $\sqrt{s}=1.8$ TeV the ratio of gluon to quark jets near $E_t^j \sim 50$ GeV must be 3:1 and must decrease slowly with increasing E_t^j (Ref. 148). The too high values of $D(z,Q^2)$ for $z<0.1$ obtained at CDF may indicate a difference between the fragmentation functions of gluon (at CDF) and quark (TASSO) jets. Comparison of the fragmentation function $D(z,Q^2)$ with the results of modeling using the HERWIG program showed that this program gives a good description of the fragmentation process in the entire range of z studied.

The CDF Collaboration also carried out a detailed comparison of the distribution of the flux E_T in the jet inside the cone described by radius R with the results of theoretical calculations. For this the function $F(r,R,E_T^j)$, which represents the r dependence of the fraction E_T^j) contained in the inner cone with $r<R$, was calculated for jets of fixed energy E_T^j. The distribution $F(r,R=1, E_T^j=100$ GeV) obtained in Ref. 159 is shown in Fig. 18. We see that it is in good agreement with the results of the perturbative QCD calculations including the α_s^3 term. In performing this analysis it was found[160] necessary to augment the theoretical description of a jet as a cone with axis along the momentum of the fragmenting parton, which was used in the perturbative QCD calculations on the basis of the Snowmass convention, by a procedure for separating two overlapping jets, similar to that used in the CDF algorithm described in Sec. 5.2.

Let us conclude this section by noting that from the viewpoint of a number of theoreticians the technique for isolating hadronic jets at pp colliders of the next generation (UNK, LHC) will need to be developed further, and the possibility of extending to hh interactions a technique similar to the k_t algorithm for e^+e^- interactions is under active study at the present time. For this, Catani *et al.*[161] have proposed the introduction of a stage of preliminary identification of "protojets," which will allow the identification of groups of hadrons related to spectator quark fragmentation, after which a modified k_t algorithm must be used for the final separation of all jets from hard subprocesses. Ellis *et al.*[162] have proposed a recursive procedure for jet identification as a function of the variable $d_{\min}$, a measure of the nearness of two "protojets," which combines several features of the JADE algorithm and the cone algorithm. This procedure makes it possible to include the effect of jet superposition in a manner which is easily reproduced in the calculation of the cross section for inclusive jet production using perturbative QCD taking into account higher-order terms.

6. JET PRODUCTION IN *ep* COLLISIONS

Since the startup in May 1992 of the ep collider HERA with colliding beams of energy 30 GeV (e)+820 GeV (p) ($\sqrt{s}\sim 300$ GeV) at DESY (Hamburg, Germany), jet production in deep-inelastic ep collisions has been studied intensively. Two large magnet detectors with 4π geometry have been built for this. One of them, ZEUS,[163] has precision sampling calorimeters made of uranium plus scintillator and a small central solenoid with a tracking system. The other, H1,[164] has liquid-argon calorimeters with iron plates and an internal tracking system located inside a large superconducting solenoid. We shall briefly describe the preliminary results on hadronic jet formation obtained for statistics of about 25 nb^{-1} collected by each of these detectors during the 1992 run.[3)]

In lowest-order perturbative QCD deep-inelastic lepton–proton scattering leads to the appearance of a single jet with large p_t corresponding to a quark knocked out by a lepton and a narrow "beam" of secondary hadrons from the fragmentation of the remnants of the proton making a large angle with the initial direction of the proton, which in the ep collider falls mainly inside the vacuum chamber. In going to higher orders of perturbative QCD two types of mechanism arise for the production of additional partons, as illustrated in Fig. 19.

In one case the photon interacts directly with a charged constituent of the target (i.e., the interaction is induced by a direct photon), and an additional parton is produced via QCD Compton scattering (Fig. 19a) or in boson–gluon fusion (Fig. 19b). In the second case the photon before interaction fragments into its constituents, one of which undergoes hard scattering on a parton of the target (this process is also referred to as interaction of a resolved photon). Here the concept of the photon structure function arises; it describes the probability of finding in the photon a parton carrying a fraction x_γ of its momentum. The photon structure function has two components: one arising from the pointlike coupling to the $\bar{q}q$ pair (Fig. 19c) and the second arising from the possibility of the photon making a transition to a bound $\bar{q}q$ state corresponding to a vector meson (Fig. 19d). This formalism is described in more detail in, for example, Ref. 165.

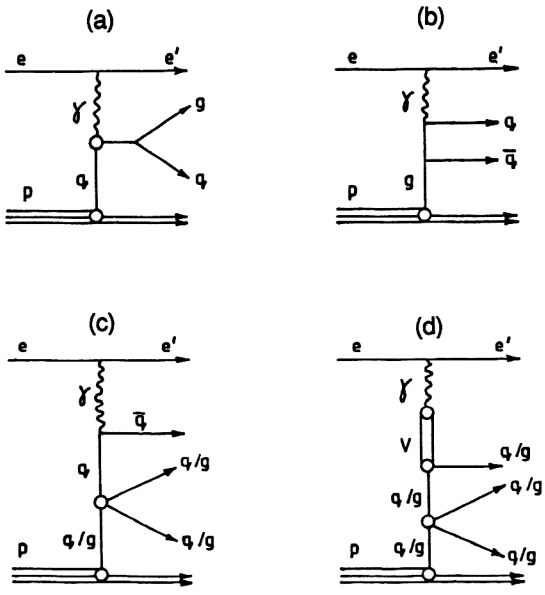

FIG. 19. Feynman diagrams for hard ep collisions described in the $O(\alpha_s^2)$ approximation of perturbative QCD.

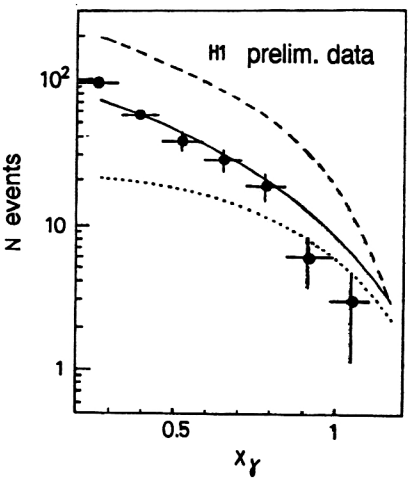

FIG. 20. Preliminary data on the photon structure function obtained at the H1 setup.

The structure of hadronic final states was studied for statistics of 3808 events with $-Q^2=(p_e-p_{e'})^2>4$ GeV^2 and $y_{JB}=(1/2)\cdot E_e\cdot\Sigma_i E_i(1-\cos\Theta_i)\geq 0.02$, (where p_e and $p_{e'}$ are the electron 4-momentum before and after the scattering), selected from the 4×10^6 triggers recorded by the ZEUS detector.[166] Jets were isolated using a cone-type algorithm with $R=1.0$ and the additional restrictions $E_j>4$ GeV and $\Theta_j>15°$. It was found that the percentages of events with 0, 1, 2, and 3 jets which did not contain jets from the fragmentation of proton fragments were 76%, 20%, 2.9%, and 0.5%, respectively. This result was in good agreement with the results of MC modeling in which processes of first order in perturbative QCD were described by the exact matrix element for the graphs in Figs. 19a and 19b, and higher orders were effectively included by the gluon cascade described in the leading-log approximation. The large number of hadron events without a hard jet was a consequence of the kinematical constraints imposed on the event selection. It was concluded in that study that in QCD the production of two jets with large transverse energy mainly occurs via Compton scattering and boson–gluon fusion. Processes with a resolved photon were not taken into account in this study.

Events from hard γp scattering were also recorded at the H1 setup. In the data analysis the H1 Collaboration from the start took into account processes with a resolved photon. The existence of a contribution from these processes was established already for the limited data processed by the end of 1992 (Ref. 167). In particular, the distribution of the energy flux in the polar angle Θ relative to the primary proton direction constructed for events with two jets and $\Theta_j<100°$ showed that a significant fraction of the flux lies in the range $140°<\Theta<180°$, in which direct photons make practically no contribution. In Fig. 20 we show the event distribution in the fraction of momentum of the resolved photon x_γ carried by the parton participating in hard scattering on a constituent parton obtained for a set of about 800 events with two jets having $E_t^j>5$ GeV (Ref. 168). In the same figure we show the results of the calculation using the photon structure function in the GRV parametrization[169] (solid line) and the LAC3 parametrization[170] (dashed line), which were obtained from analysis of $\gamma\gamma$ interactions at e^+e^- colliders. As is well known, this type of interaction permits reconstruction of the quark distribution in the photon, but gives little information about the gluon distribution. Therefore, the parametrizations of the gluon distributions obtained by different authors in analyzing $\gamma\gamma$ collisions differ considerably. For example, the LAC3 parametrization assumes a large gluon component for $x_\gamma>0.2$, which clearly contradicts the experimental distribution. On the other hand, the assumption that the gluon component in the photon is completely absent also disagrees with experiment. Therefore, the preliminary data on the x_γ distribution obtained in the H1 experiment at least indicate that the gluon component of the photon can be measured accurately in hard γp collisions.

The H1 detector also saw events in which between the hadronic jets and the primary proton direction there is a large ($\eta>1.8$) pseudorapidity interval not containing hadrons with energy greater than 0.4 GeV (Ref. 168). These events can be produced in hard photon–Pomeron interactions, which can give information about the Pomeron structure function.[171]

7. JET SPECTROSCOPY

The experimentally established fact that the kinematical parameters of the generating partons can be fairly accurately reconstructed from measurements of jets with large E_t^j makes it possible to use jets for reconstructing the invariant mass of two and more partons. This possibility attracted the particular attention of experimentalists, when the problems of accurate measurement of the W-boson mass, for which the hadronic decay mode is dominant (67.6%), and of searching for new particles decaying into $W^\pm$ arose. Although the technique of determining the masses of new particles from the peak in the invariant-mass spectrum of their decay products has been used in high-energy physics already for several de-

cades now and has been studied carefully, going from the calculation of the invariant masses of several individual hadrons (or leptons) to the analogous calculations using jets required additional technical studies. This nascent field, referred to as jet spectroscopy, has survived its birth and the main results given below have been obtained for modeled events in preparation for experiments to be carried out at the next generation of e^+e^- and hh colliders.

7.1. The jet spectroscopy of vector gauge bosons

7.1.1. Measurement of the W-boson mass in e^+e^- annihilation

The problem of measuring the W-boson mass using its hadronic decay products was first studied in 1978 (Ref. 172) in preparation for the research to be carried out at LEP II. It was noticed that in W-boson pair production via the reaction

$$e^+e^- \to W^+W^- \tag{19}$$

for the accurate measurement of m_W it is preferable to use the 4-jet final state from the hadronic decays of two Ws, since the absence of other sources of jets in (19) makes it possible to use kinematical constraints. The problem of the kinematical analysis of four-jet final states in e^+e^- annihilation was studied in a more general form by Wu.[173] Detailed modeling of the accuracy of reconstructing m_W in reaction (19) for the existing experimental setups at LEP II (Ref. 174) showed that when the direct results of measurements of the kinematical jet parameters using calorimeters are used to calculate the invariant mass $M(2j)$, the W boson peak is shifted by several GeV to smaller masses owing to loss of the part of the jet energy carried by μ mesons and neutrinos, and also owing to the finite size of the cone describing the jet. However, if, neglecting radiation losses of W bosons, a kinematical fit is made of the parameters of four (or five in the case where quarks from W-boson decay emit a bremsstrahlung gluon) jets imposing the condition that within the energy resolution of the calorimeters the total 3-momenta of two combinations of two (three) jets balance each other and the total jet energy is equal to the energy of the colliding beams, the accuracy of determining m_W is raised to 100 MeV. It has also been established that the uncertainty in reconstructing m_W using this procedure depends rather weakly on how accurate the calorimeters are. However, accurate measurement of the W-boson width from the peak in the invariant-mass spectrum is impossible even at e^+e^- colliders.

7.1.2. The technique of identifying gauge bosons using their hadronic decay modes at hh colliders

The need to identify the W boson at hadron colliders from the invariant mass $M(2j)$ of the jets from their decay is dictated by the requirements of using the jet spectroscopy technique to isolate the signal from heavier objects decaying into W bosons (primarily $t \to Wb$ and $H^0 \to W^+W^-$) under very complicated background conditions. However, at hadron colliders the problems of jet spectroscopy are made considerably more complicated by the two following factors. First, the cross section for jet production in parton hard-scattering subprocesses is several orders of magnitude greater than the cross section for W-boson production, which generates a large background in the $M(2j)$ spectra. Second, the complexity of the final state with a W boson or with another heavy particle having hadronic decay modes makes it impossible to use constraints which improve the accuracy of the resolution in the invariant mass of two and more jets. Therefore, in designing detectors for hadronic colliders of the next generation care has been taken to understand the requirements on their characteristics which will ensure a resolution in the W-boson invariant mass $M(2j)$ adequate for seeing a peak in the $M(2j)$ spectrum under the conditions of high background from the processes (11). Here wide use has been made of the experience gained in the successful isolation of the W and Z^0 signal in the $M(2j)$ spectrum in the UA2 experiment for $\sqrt{s}=630$ GeV, which will be studied below.

The first indications of the existence in the $M(2j)$ spectrum of a signal from the hadronic decay of the W and Z^0 in this setup were obtained already at the initial stage of processing statistics of 0.73 pb^{-1} (Ref. 175). The definitive results were obtained using the modernized setup for statistics of 4.7 pb^{-1} (Ref. 176). In this study the $M(2j)$ spectrum was analyzed by selecting events with the two jets of highest energy lying in the range $|\eta|<0.6$, for which the transverse energy of any of the additional jets is not greater than 20 GeV. The results of the modeling showed that the best resolution in $M(2j)$ is obtained when the jet is described by a cone with $R=0.8$. The resulting distribution $d\sigma/dM(2j)$ was approximated by a smooth function describing the shape of the background from processes (11) and the sum of two Gaussians to take into account the peaks from W- and Z^0-boson decay. In the approximation m_W was assumed to be a free parameter, and $m_Z=1.13m_W$ on the basis of accurate measurements of the masses of the vector gauge bosons made by the UA2 Collaboration.[177] The cross section for W-boson production was also determined by a fit, and the ratio of the signals W/Z was taken to be 0.397 on the basis of the measured cross sections of these bosons and the modeling of the detector acceptances. The approximation gave the following estimate of the cross section: $\sigma \cdot B(W,Z \to q\bar{q}) = 9.6 \pm 2.3$ (stat.) $+1.1$ (syst.), which is 1.6 times greater than the cross section calculated in $O(\alpha_s^2)$ perturbative QCD. The estimate obtained for the resolution in the invariant mass $(9.9 \pm 2.5)\%$ is in good agreement with that expected from the modeling $(10.7 \pm 1.8)\%$.

In Fig. 21 we show the distribution in $M(2j)$ in the region of the W and Z bosons obtained after subtraction of the smooth background. We see that the experimental resolution of UA2 is insufficient to distinguish the peaks from the W and Z^0 bosons. However, this distribution permits a fairly accurate estimate of the W-boson mass: $m_W=79.2 \pm 1.7$ GeV.

Using the complete statistics of the experiment, 10.9 pb^{-1}, the UA2 Collaboration carried out a search for heavy vector gauge bosons according to their decays into two jets, $W_R \to \bar{q}q$ and $Z' \to \bar{q}q$. A technique analogous to that described above was used to seek their signals in the invariant-mass spectrum $M(2j)$. It was found that at the 90% confidence level $M(W_R)>251$ GeV and $M(Z')>237$ GeV (Ref. 114).

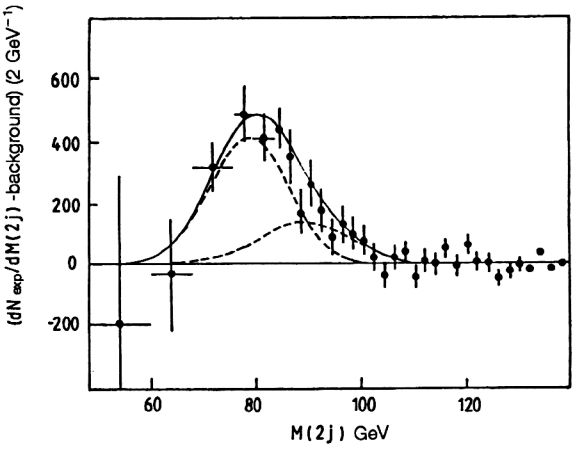

FIG. 21. Distributions in $M(2j)$ near the W and Z^0 bosons obtained at the UA2 setup after subtracting the smooth background function. The solid line shows the result of the approximation by the sum of two Gaussians (dashed lines) for the W and Z^0 bosons.

In designing calorimeters for setups with 4π geometry at the energies of the next generation of colliders it has become common to optimize such calorimeters in the width of the invariant-mass peaks of the two jets from hadronic decays of W and Z^0 bosons. The authors of Ref. 178 carried out a detailed study of the effects influencing the resolution in the invariant mass of the W boson at $\sqrt{s}=40$ TeV. Events of the reaction

$$pp\rightarrow W+nj+X \tag{20}$$

were modeled using the ISAJET program. Additional uncertainties mimicking the results of measurements using calorimeters with various accuracies were introduced into the kinematical parameters of the modeled jets from hadronic decays of the W, which were described by a cone with $R=0.7$. It was shown that the resolution in the W mass depends weakly on the energy resolution of the calorimeters, but rapidly worsens with cell dimensions greater than $\Delta\varphi\cdot\Delta\eta=0.1\cdot 0.1$. It was also shown in this study that an axially symmetric magnetic field of strength $H=3T$ in the central region of the calorimeter significantly (by a factor of 1.5) worsens the resolution in the W mass. This resolution also falls significantly when several "soft" background events are superimposed on an event containing a W boson, which is unavoidable in hadron colliders with high luminosity.

7.2. Problems in measuring the t-quark mass

The partner of the b quark in the $SU(2)$ doublet, the t quark, is now obviously the last undiscovered quark. Although there is already a great deal of indirect experimental data[179,180] providing evidence of a heavy (i.e., with $m_t>m_W$) t quark, the direct discovery of the t quark from its decay products and the accurate measurement of m_t are among the most important problems in high-energy physics. Since in the minimal standard model (i.e., the model not containing charged Higgs bosons) the t quark always decays with the emission of a real W boson, the three following final-state configurations from $t\bar{t}$-pair decay are possible depending on the W decay mode:

$$t\bar{t}\rightarrow(l^+\nu b)(l^-\bar{\nu}\bar{b}) \tag{21}$$

$$t\bar{t}\rightarrow(q\bar{q}b)(l^-\bar{\nu}\bar{b}) \tag{22}$$

(plus the charge-conjugate configuration)

$$t\bar{t}\rightarrow(q\bar{q}b)(q\bar{q}\bar{b}). \tag{23}$$

The probabilities of these configurations obey the ratio 1:4:4.

7.2.1. Accuracy of measuring the invariant mass of the t quark at e^+e^- colliders

Since t-quark decay involves a W boson, the accurate reconstruction of its invariant mass at the e^+e^- collider is made easier by the factors described in Sec. 7.1.1. Discovery of the t quark in e^+e^- annihilation is possible only at the future linear e^+e^- colliders with $\sqrt{s}\geq 500$ GeV (VLEPP, JLC), and a great deal of attention has been paid to this problem in developing a program for research for the new generation of colliders. The analysis of the background conditions carried out in Ref. 181 showed that for $m_t\sim 150$ GeV the main source of background is W-boson pair production, the cross section for which at $\sqrt{s}\sim 400$ GeV is about 10 times greater than the cross section for $t\bar{t}$-pair production. However, this background can easily be eliminated using the standard technique of kinematical fitting. In that study a measurement accuracy of $\sigma(m_t)\leq 0.5$ GeV was obtained. This accuracy was later confirmed in Ref. 182 on the basis of detailed modeling of the process (23).

However, the main hopes for precision determination of the t-quark mass at e^+e^- colliders are related to measurement of the energy dependence of $\sigma(t\bar{t})$ in the near-threshold region,[183] so the technique of string spectroscopy is viewed as auxiliary.

7.2.2. Possibilities of measuring the t-quark mass at hadron colliders

Detailed study of the possibilities of finding the t quark at FNAL energies[184] has shown that detection of its decay signal in the strong background of other hard interactions is possible using $(e\mu)$ pairs from the state (21) or by the selection of events with a hard isolated lepton and with three or more jets from the state (22). The purely hadronic decay of the $t\bar{t}$ pair cannot be distinguished owing to the background of multijet events from hard scattering of partons, the production cross section for which exceeds the cross section for $t\bar{t}$-pair production by several orders of magnitude. Therefore, the hopes of measuring the t-quark mass at hadron colliders of the new generation are usually pinned on the state (22), for which the leptonic decay of the t quark can be used to isolate events containing a $t\bar{t}$ pair from the background, and the t-quark mass can be calculated using hadronic decay.

A detailed study of the accuracy of measuring m_t which can be attained at a hadron collider for $\sqrt{s}=6$ TeV has been carried out in Refs. 185, 186, 187, and 188 as part of the development of a program of scientific research for the UNK collider. In Ref. 186 the program ISAJET was used to model

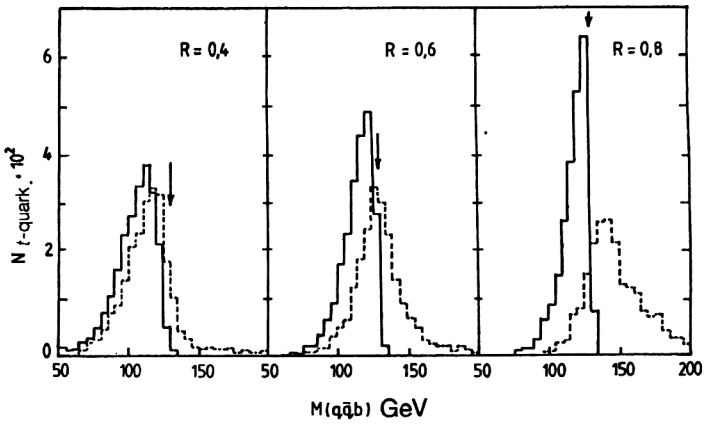

FIG. 22. R dependence of the distributions in the invariant mass $M(q\bar{q}b)$ for various jet identification procedures (see the text).

5000 events of reaction (22), of which only 2450 passed all the selection criteria applicable in an experiment to isolate this final state ($\Sigma E_t > 150$ GeV, $E_t^{\text{missing}} > 20$ GeV, an isolated lepton with $E_t > 20$ GeV, $n_j > 3$ for $E_t^j > 20$ GeV). Detailed study of the properties of bremsstrahlung gluon emission has shown that in each event an average of five gluon jets with $E_t^j > 5$ GeV appears, where four of these are emitted by partons of the initial state. In selecting hard jets with $E_t^j > 20$ GeV an average of 1.6 gluon jets remain per event, and for those with quark jets about 5 hard jets remain, which increases the combinatorial background. Combined with the low energy resolution in the invariant mass $M(q\bar{q}b)$ of the products of t-quark decay induced by gluon emission of final-state partons, underestimation of the jet energy owing to muons and neutrinos undetected by the calorimeters and also the superposition of jets and hadronic background from spectator parton fragmentation, this leads to a signal-to-background ratio which makes it impossible to isolate the t-quark peak in the invariant-mass spectrum $M(3j)$ (Ref. 187).

In Ref. 188 it was shown that the relative contribution of the effects listed above varies as the radius R of the cone used to describe the jet is changed, which makes it possible to optimize the resolution in $M(3j)$ by selecting the value of R. In Fig. 22 we show the distributions in $M(q\bar{q}b)$ for the set of modeled events described above obtained for three values of R. The solid-line histograms correspond to the distributions obtained by including only particles from quark fragmentation (tagged in ISAJET) which fell into the cone, and the dashed-line histograms correspond to the distributions obtained including all the particles in the cone. Although these distributions were constructed neglecting the distortions introduced by the calorimeters, the widths of the distributions are considerably larger than the width $\Gamma_t = 0.7$ GeV obtained in the modeling of t quarks. As R increases the $M(2j)$ distribution for the fragmentation particles narrows and its peak approaches the value obtained in the modeling $m_t = 130$ GeV, but the distribution corresponding to the actual definition of the jet is shifted to the right and for $R > 0.6$ begins to broaden. Additional analysis showed that the shift of the maximum of the distribution is due to the contribution of the background of soft hadrons nearly uniformly distributed in $\eta - \varphi$ space, and the broadening of the distribution is related to large fluctuations in the measured value of m_t induced by superpositions of fairly hard gluon jets. At the energy studied the probability of such superposition for jets from quarks $q, \bar{q}$ from t-quark decay is 40%. Therefore, in invariant-mass studies at hadronic colliders with $\sqrt{s} \geq 6$ TeV it is necessary to use a new jet recognition procedure which minimizes cases of overlap.

A version of such an algorithm has been developed and tested for modeled events in Refs. 186 and 188. For brevity we shall refer to this as the KM algorithm, from the names of its authors. The special features of the KM algorithm compared to the algorithms described above for the recognition of individual jets are the following:

- First the distance d_0 between the centers of the two jets at which the jets first become distinguishable is introduced; if $d < d_0$ the jets from two partons are combined to form a single jet;
- Distinguishable jets are assumed to be overlapping if $d < 2R$; otherwise the jets are assumed to be isolated (an i.j.). Overlap of only two jets (t.j.) and three jets (th.j.) is allowed for. Events with four or more overlapping jets are rejected;
- The invariant mass of the t quark is calculated for configurations $t \to 3(i.j)$, $t \to (i.j.) + (t.j.)$, $t \to (th.j.)$; the energy and 3-momentum of the two- and three-jet configurations are determined from the particles (or calorimeter cells) falling in the region bounded by superimposed circles of radius R, i.e., without real resolution of the overlapping jets.

Thus, instead of criteria for separating jets, the KM algorithm contains criteria for distinguishing them, so that to calculate the invariant masses of n jets it is necessary only to be able to determine the number of jets and the calorimeter region occupied by them.

In Fig. 23 we show the R dependences of the widths of the peaks in the effective-mass spectra of the W boson and t quark obtained by approximating these peaks by an asymmetric Breit–Wigner function for the cases described above of taking into account all particles falling into the cone, and only for daughter particles. We see the above-noted tendency for the peak to broaden with increasing R in the first case, and for it to narrow significantly in the second. The open circles in this figure show the R dependences of the widths obtained for a sample of individual and overlapping jets selected using the KM algorithm. The procedure proposed for

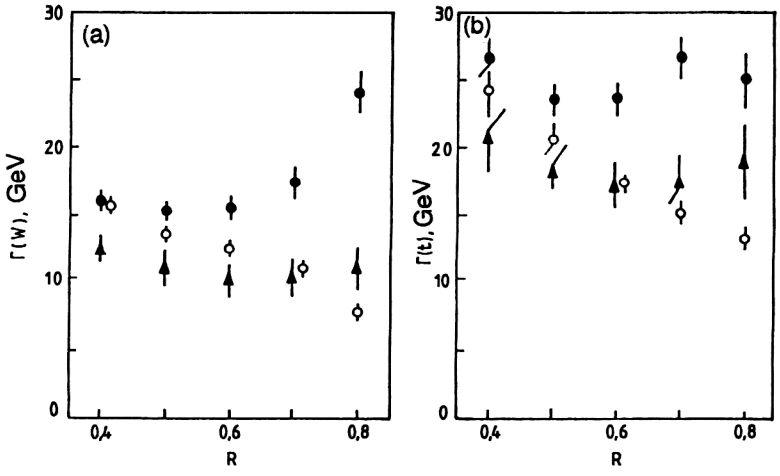

FIG. 23. R dependence of the W-boson and t-quark widths obtained for various jet definitions (see the text).

processing overlapping jets leads to a noticeable (by one and a half times for $R=0.7$) improvement of the resolution in the invariant mass. A noticeable peak from the t quark has appeared as a result of this and the decrease of the combinatorial background in the invariant-mass distribution $M(3j)$. Approximation of this peak by an asymmetric Breit–Wigner function plus a smooth function obtained in the approximation of the modeled combinatorial background for various accuracy characteristics of the calorimeters at several values of R has shown that the energy resolution of the calorimeters is not especially important for the resolution in $M(3j)$ near the t-quark peak. As a result of analysis of the R dependence of the estimate of m_t in Ref. 188 it was concluded that in hadron colliders the t-quark mass cannot be measured with an error of less than 3 GeV.

The study of the accuracy of measuring m_t from the invariant mass $M(3j)$ carried out in Ref. 189 for the LHC energy gave the estimate $\Delta m_t \sim 8$ GeV. Therefore, in Ref. 190 it was suggested that the "toponium" mass be measured at LHC using its decay into 2γ, which makes it possible to estimate m_t with an accuracy of up to ~100 MeV. However, these measurements are possible only for $m_t < 120$ GeV.

8. CONCLUSION

During the last 15 years the study of hadronic jets arising in DEPs has become an entirely new area in high-energy physics. This area began to develop especially rapidly after the construction of high-energy e^+e^- and hh colliders. The results of numerous studies in jet physics carried out at these colliders have impressively confirmed the correctness of the fundamental ideas of QCD.

It follows from the experimental data that we have discussed in this review that the cleanest conditions for studying jets exist at e^+e^- storage rings. Unfortunately, this accelerator technology has strong energy limitations, and for the next generation of e^+e^- colliders (VLEPP, JLC) there are plans to use the technology of linear colliders, which means that some of the advantages of e^+e^- storage rings are lost. However, even at these e^+e^- colliders the technique of jet spectroscopy ensures an accuracy in measuring the masses of new heavy particles considerably better than that obtainable at hh colliders. But still, from the viewpoint of going to higher energies, the real hopes are pinned on pp colliders of the next generation (UNK, LHC), where jet physics will become the testing ground for detailed verification of the higher orders of perturbative QCD, and the technique of jet spectroscopy will be used as a tool for searching for new heavy particles.

[1)]The name of the program is an abbreviation of Hadron Emission Reactions With Interfering Gluons.
[2)]There is also a modification of this algorithm in which $E^2_{\rm vis}$ is used instead of s.
[3)]These statistics were increased by a factor of 20 in the 1993 run.

[1] F. J. Yndurian, *Quantum Chromodynamics: An Introduction to the Theory of Quarks and Gluons* (Springer, New York, 1983).
[2] P. Darriulat, Ann. Rev. Nucl. Part. Sci. **30**, 159 (1980).
[3] A. Casher *et al.*, Phys. Rev. Lett. **31**, 792 (1973).
[4] R. D. Field and R. Feynman, Phys. Rev. D **15**, 2590 (1977).
[5] R. D. Field and R. Feynman, Nucl. Phys. **B79**, 355 (1979).
[6] A. Ali *et al.*, Phys. Lett. **93B**, 115 (1980).
[7] T. Meyer, Z. Phys. C **12**, 77 (1982).
[8] B. Andersson *et al.*, Phys. Rep. **97**, 31 (1983).
[9] M. Bengtsson and T. Sjostrand, Phys. Lett. **185B**, 435 (1987).
[10] Z. Kunszt and W. J. Stirling, Phys. Lett. **171B**, 307 (1986).
[11] G. Altarelli and G. Parisi, Nucl. Phys. **B126**, 298 (1977).
[12] K. Konishi *et al.*, Phys. Lett. **78B**, 243 (1974).
[13] D. Amati and G. Veneziano, Phys. Lett. **83B**, 87 (1979).
[14] B. N. Ermolaev and V. S. Fadin, Pis'ma Zh. Eksp. Teor. Fiz. **33**, 285 (1981) [JETP Letters **33**, 269 (1981)].
[15] V. S. Fadin, Yad. Fiz. **37**, 408 (1983) [Sov. J. Nucl. Phys. **37**, 245 (1983)].
[16] A. Basseto *et al.*, Nucl. Phys. **B207**, 189 (1982).
[17] A. H. Mueller, Phys. Rep. **73**, 237 (1981).
[18] A. H. Mueller, in *Proc. of the Workshop on Jet Physics at LEP and HERA*, Durham, England (1990), p. A1.
[19] Yu. L. Dokshitzer *et al.*, Phys. Lett. **115B**, 242 (1982).
[20] Ya. I. Azimov *et al.*, Pis'ma Zh. Eksp. Teor. Fiz. **35**, 390 (1982) [JETP Letters **35**, 482 (1982)].
[21] Yu. L. Dokshitser and S. I. Troyan, Preprint No. 922, Leningrad Nuclear Physics Institute, Gatchina (1984) [in Russian].
[22] Yu. L. Dokshitzer *et al.*, Rev. Mod. Phys. **60**, 373 (1988).
[23] D. Amati and G. Veneziano, Phys. Lett. **83B**, 87 (1979).
[24] C. P. Fong and B. R. Webber, Phys. Lett. **299B**, 289 (1989).
[25] E. A. Kuraev, L. N. Lipatov, and V. S. Fadin, Zh. Eksp. Teor. Fiz. **72**, 377 (1977) [Sov. Phys. JETP **45**, 199 (1977)].
[26] Ya. Ya. Balitskiĭ and L. N. Lipatov, Yad. Fiz. **28**, 822 (1978) [Sov. J. Nucl. Phys. **28**, 1597 (1978)].
[27] L. B. Gribov, E. M. Levin, and M. G. Riskin, Phys. Rep. **100**, 1 (1983).
[28] C. P. Fong and B. R. Webber, Phys. Lett. **241B**, 255 (1990).
[29] C. Peterson *et al.*, Phys. Rev. D **27**, 105 (1983).
[30] F. Paige and S. Protopopescu, Report BN-38034, Brookhaven (1986).
[31] G. C. Fox and S. Wolfram, Nucl. Phys. **B168**, 285 (1980).
[32] T. Sjostrand, Phys. Lett. **157B**, 321 (1985).
[33] F. A. Berends *et al.*, Phys. Lett. **224B**, 237 (1989).

[34] G. Marchesini and B. R. Webber, Nucl. Phys. **B310**, 461 (1988).
[35] R. K. Ellis *et al.*, Nucl. Phys. **B286**, 643 (1987).
[36] M. Bengtsson *et al.*, Phys. Lett. **185B**, 435 (1987).
[37] R. Odorico, Comput. Phys. Commun. **32**, 687 (1984).
[38] B. Van Eijk, Preprint CERN-EP/85-121, CERN, Geneva (1985).
[39] J. D. Bjorken and S. J. Brodsky, Phys. Rev. D **1**, 1416 (1970).
[40] E. Farhi, Phys. Rev. Lett. **39**, 1587 (1977).
[41] M. J. Counihan, Phys. Lett. **59B**, 367 (1975).
[42] H. Georgi and M. Machacek, Phys. Rev. Lett. **39**, 1237 (1977).
[43] S. Brandt and H. D. Dahmen, Z. Phys. C **1**, 61 (1979).
[44] G. C. Fox and S. Wolfram, Phys. Rev. Lett. **41**, 1581 (1978).
[45] A. M. Baldin *et al.*, Yad. Fiz. **41**, 995 (1985) [Sov. J. Nucl. Phys. **41**, 639 (1985)]; **48**, 841 (1988) [**48**, 536 (1988)].
[46] G. Hanson *et al.*, Phys. Rev. Lett. **35**, 1609 (1975).
[47] W. Bartel *et al.*, Phys. Lett. **91B**, 142 (1980).
[48] Ch. Berger *et al.*, Phys. Lett. **91B**, 418 (1980).
[49] R. Brandelik *et al.*, Phys. Lett. **86B**, 943 (1979).
[50] D. P. Barber *et al.*, Phys. Rev. Lett. **43**, 830 (1979).
[51] J. Ellis and I. Karliner, Nucl. Phys. **B148**, 141 (1979).
[52] G. Kramer *et al.*, Phys. Lett. **79B**, 249 (1978).
[53] F. A. Berend and R. Kleiss, Report 80/73, DESY, Hamburg (1980).
[54] J. Ellis *et al.*, Nucl. Phys. **B111**, 253 (1976).
[55] R. Brandelik *et al.*, Phys. Lett. **97B**, 453 (1980).
[56] P. Hoyer *et al.*, Nucl. Phys. **B161**, 349 (1979).
[57] Ch. Berger *et al.*, Phys. Lett. **97B**, 459 (1980).
[58] H. J. Behrend *et al.*, Phys. Lett. **110B**, 329 (1982).
[59] G. Sterman and S. Weinberg, Phys. Rev. Lett. **39**, 1436 (1977).
[60] T. Sjostrand, Comput. Phys. Commun. **28**, 229 (1983).
[61] W. Bartel *et al.*, Z. Phys. C **33**, 23 (1986).
[62] B. Flaugher, Fermilab-Conf-90/248-E (1990).
[63] S. Catani *et al.*, Phys. Lett. **269B**, 432 (1991).
[64] B. R. Webber, Preprint CERN-TH.6706/92, CERN, Geneva (1992).
[65] G. Kramer and B. Lampe, Z. Phys. C **39**, 101 (1988).
[66] K. Abe, Preprint 90-23, KEK, Japan (1990).
[67] P. D. Acton *et al.*, Preprint CERN-PPE/92-18, CERN, Geneva (1992).
[68] M. Z. Akrawy *et al.*, Z. Phys. C **49**, 375 (1991).
[69] G. Altarelli, Preprint CERN-TH.6623/92, CERN, Geneva (1992).
[70] M. Z. Akrawy *et al.*, Phys. Lett. **235B**, 389 (1990).
[71] B. Adeva *et al.*, Phys. Lett. **248B**, 464 (1990).
[72] P. Abreu *et al.*, Phys. Lett. **247B**, 167 (1990).
[73] D. Decamp *et al.*, Preprint CERN-PPE/90-176, CERN, Geneva (1990).
[74] Yu. L. Dokshitzer and M. Olsson, Preprint LU TP92-17, Lund University (1992).
[75] S. Catani *et al.*, Preprint Cavendish-HEP-91/12, Cambridge University (1991).
[76] S. Bethke *et al.*, Preprint CERN-PPE/91-36, CERN, Geneva (1991).
[77] A. Ali *et al.*, Nucl. Phys. **B167**, 454 (1980).
[78] S. Bethke *et al.*, Z. Phys. C **49**, 59 (1991).
[79] O. Nachtmann and A. Reuter, Z. Phys. C **16**, 45 (1982).
[80] P. Abreu *et al.*, Phys. Lett. **255B**, 466 (1991).
[81] P. Abreu *et al.*, Preprint CERN-PPE/93-29, CERN, Geneva (1993).
[82] D. Decamp *et al.*, Phys. Lett. **279B**, 411 (1992).
[83] M. Altoff *et al.*, Z. Phys. **22**, 307 (1984).
[84] M. Z. Akrawy *et al.*, Phys. Lett. **247B**, 617 (1990).
[85] P. D. Acton *et al.*, Preprint CERN-PPE/92-89, CERN, Geneva (1992).
[86] M. Altoff *et al.*, Z. Phys. C **29**, 347 (1985).
[87] A. Petersen *et al.*, Phys. Rev. Lett. **55**, 1954 (1985).
[88] W. Braunschweig *et al.*, Z. Phys. C **45**, 1 (1989).
[89] W. Bartel *et al.*, Phys. Lett. **123B**, 460 (1983).
[90] R. J. Madaras *et al.*, in *Recontre de Moriond on Strong Interactions and Gauge Theories*, Les Arcs (1980).
[91] Y. K. Kim *et al.*, Preprint 90-79, KEK, Japan (1990).
[92] G. Alexander *et al.*, Phys. Lett. **265B**, 462 (1991).
[93] P. D. Acton *et al.*, Preprint CERN-PPE/93-02, CERN, Geneva (1993).
[94] AFS Collaboration, in *Proc. of the Twenty-First Intern. Conf. on High Energy Physics*, Paris, 1982; J. Phys. **43**, C3-122 (1982).
[95] H. Gordon *et al.*, Nucl. Instrum. Methods **196**, 303 (1982).
[96] T. Akesson *et al.*, Phys. Lett. **121B**, 133 (1983); **128B**, 354 (1983).
[97] A. L. Angelis *et al.*, Phys. Lett. **126B**, 132 (1983).
[98] M. Barranco Luque *et al.*, Nucl. Instrum. Methods **176**, 175 (1980).
[99] M. Calvetti *et al.*, Nucl. Instrum. Methods **176**, 255 (1980).
[100] K. Eggert *et al.*, Nucl. Instrum. Methods **176**, 213 (1980).
[101] M. Albrow *et al.*, Preprint CERN-EP/87-55, CERN, Geneva (1987).
[102] A. Beer *et al.*, Nucl. Instrum. Methods **224**, 360 (1984).
[103] M. Dialinas *et al.*, Preprint LAL-RT/83-14, Orsay (1983).
[104] C. Conta *et al.*, Nucl. Instrum. Methods **224**, 65 (1984).
[105] K. Borer *et al.*, Nucl. Instrum. Methods **224**, 29 (1984).
[106] F. Bosi *et al.*, Nucl. Instrum. Methods A **283**, 532 (1989).
[107] R. Ansari *et al.*, Nucl. Instrum. Methods A **279**, 388 (1989).
[108] R. Ansari *et al.*, Nucl. Instrum. Methods A **263**, 51 (1988).
[109] J. Alitti *et al.*, Nucl. Instrum. Methods A **279**, 364 (1989).
[110] E. Abe *et al.*, Nucl. Instrum. Methods A **271**, 387 (1988).
[111] D. Crane, Preprint FERMILAB-Conf-91/238-E, Fermilab, Batavia (1991).
[112] B. Pifer *et al.*, DO Design Report, FERMILAB Internal Report, November, 1993.
[113] M. Abolins *et al.*, Nucl. Instrum. Methods A **280**, 36 (1989).
[114] J. Alitti *et al.*, Preprint CERN-PPE/93-66, CERN, Geneva (1993).
[115] B. L. Combridge *et al.*, Phys. Lett. **70B**, 234 (1977).
[116] R. Cutler and D. Sivers, Phys. Rev. D **17**, 196 (1978).
[117] Z. Kunszt and E. Pietarinen, Nucl. Phys. **B164**, 45 (1980).
[118] T. Gottschalk and D. Sivers, Phys. Rev. D **21**, 102 (1981).
[119] G. Arnison *et al.*, Phys. Lett. **118B**, 167 (1982).
[120] J. A. Appel *et al.*, Z. Phys. C **30**, 341 (1986).
[121] M. Banner *et al.*, Phys. Lett. **118B**, 203 (1982).
[122] G. Arnison *et al.*, Phys. Lett. **123B**, 115 (1983).
[123] F. Abe *et al.*, Phys. Rev. Lett. **62**, 613 (1989).
[124] P. Bagnaia *et al.*, Phys. Lett. **138B**, 430 (1984).
[125] R. Ellis and J. Sexton, Nucl. Phys. **B296**, 445 (1986).
[126] J. E. Huth, Preprint FERMILAB-Conf-90/249-E, Fermilab, Batavia (1990).
[127] G. Arnison *et al.*, Phys. Lett. **132B**, 214 (1983).
[128] J. Appel *et al.*, Phys. Lett. **160B**, 349 (1985).
[129] J. Alitti *et al.*, Phys. Lett. **235B**, 363 (1990).
[130] F. Abe *et al.*, Phys. Rev. Lett. **68**, 1104 (1992).
[131] P. Harriman *et al.*, Phys. Rev. D **42**, 798 (1990).
[132] E. Eichten *et al.*, Phys. Rev. D **50**, 811 (1983).
[133] F. Abe *et al.*, Phys. Rev. Lett. **70**, 1376 (1993).
[134] S. M. Bergman *et al.*, Phys. Rev. D **4**, 3388 (1971).
[135] C. Rubbia, Preprint CERN-EP/84-55, CERN, Geneva (1984).
[136] G. Arnison *et al.*, Phys. Lett. **136B**, 294 (1984).
[137] J. C. Collins and D. E. Soper, Phys. Rev. D **16**, 2219 (1977).
[138] N. G. Antoniou, Phys. Lett. **128B**, 257 (1983).
[139] H. Abramowicz *et al.*, Z. Phys. C **12**, 289 (1982).
[140] P. Bagnaia *et al.*, Phys. Lett. **144B**, 283 (1984).
[141] B. Flaugher, Preprint FERMILAB-Conf-91/235-E, Fermilab, Batavia (1991).
[142] F. Abe *et al.*, Preprint FERMILAB-Pub-89/206-E, Fermilab, Batavia (1989).
[143] F. Berends *et al.*, Phys. Lett. **103B**, 124 (1981).
[144] J. C. Collins and D. E. Soper, Phys. Rev. D **16**, 2219 (1977).
[145] G. Arnison *et al.*, Phys. Lett. **158B**, 494 (1985).
[146] B. Andersson *et al.*, Phys. Rep. **97**, 31 (1983).
[147] R. Ansari *et al.*, Z. Phys. C **36**, 175 (1987).
[148] E. Eichten *et al.*, Rev. Mod. Phys. **56**, 574 (1984).
[149] Z. Kunszt *et al.*, Nucl. Phys. **B164**, 45 (1980).
[150] F. Abe *et al.*, Preprint FERMILAB-Pub-9/181-E, Fermilab, Batavia (1991).
[151] J. Alitti *et al.*, Phys. Lett. **268B**, 145 (1991).
[152] S. M. Berman *et al.*, Phys. Rev. D **4**, 3388 (1971).
[153] C. Rubbia, Preprint CERN-EP/84-55, CERN, Geneva (1984).
[154] C. Albajar, Z. Phys. C **36**, 33 (1988).
[155] P. Bagnaia *et al.*, Phys. Lett. **144B**, 291 (1984).
[156] J. C. Collins and D. E. Soper, Phys. Rev. D **16**, 2219 (1977).
[157] F. Abe *et al.*, Phys. Rev. Lett. **65**, 968 (1990).
[158] G. Altarelli, Phys. Rep. **81**, 1 (1982).
[159] F. Abe *et al.*, Phys. Rev. Lett. **70**, 713 (1993).
[160] S. D. Ellis, Preprint CERN-TH.6861/93, CERN, Geneva (1993).
[161] S. Catani *et al.*, Preprint CERN-TH.6775/93, CERN, Geneva (1993).
[162] S. D. Ellis and D. E. Soper, Preprint CERN-TH.6860/93, CERN, Geneva (1993).
[163] H1 Collaboration, Technical Proposal for the H1 Detector (1986).
[164] ZEUS Collaboration, The ZEUS Detector, Technical Proposal (1986).
[165] H. Abramowicz *et al.*, Preprint 91-057, DESY, Hamburg (1991).
[166] M. Derrick *et al.*, Phys. Lett. **306B**, 158 (1993).
[167] G. Wolf, Preprint 92-190, DESY, Hamburg (1992).
[168] A. De Roeck, Preprint 94-005, DESY, Hamburg (1994).
[169] M. Gluck *et al.*, Phys. Rev. D **46**, 1973 (1992).

[170] H. Abramowicz *et al.*, Phys. Lett. **269B**, 458 (1991).
[171] M. G. Ryskin, Yad. Fiz. **53**, 1077 (1991) [Sov. J. Nucl. Phys. **53**, 668 (1991)].
[172] R. Banner *et al.*, Preprint CERN-79-02/93, CERN, Geneva (1979).
[173] S. L. Wu, Z. Phys. C **9**, 329 (1981).
[174] C. Roudeau *et al.*, in *Proc. of the ECFA Workshop on LEP200*, ECFA 87/108 (1987), p. 49.
[175] R. Ansari *et al.*, Phys. Lett. **186B**, 452 (1987).
[176] J. Alitti *et al.*, Z. Phys. C **49**, 17 (1991).
[177] J. Alitti *et al.*, Phys. Lett. **249B**, 150 (1990).
[178] J. Freeman *et al.*, Preprint FERMILAB-TM-1270, Fermilab, Batavia (1990).
[179] V. Barger *et al.*, Phys. Lett. **194B**, 312 (1987).
[180] W. Bartel *et al.*, Phys. Lett. **146B**, 437 (1984).
[181] A. M. Moiseev, in *Proc. of the 1st All-Union Working Meeting on Physics at VLEPP*, Vol. 1, p. 99 (1991) [in Russian].
[182] K. Fujii, in *Proc. of the Intern. Workshop on Physics and Experiments With Linear Colliders*, Saariselka, Finland (1991).
[183] K. Fujii, Preprint 90-187, KEK, Japan (1991).
[184] H. Baer *et al.*, Phys. Rev. D **39**, 3310 (1989).
[185] A. E. Kiryunin and A. M. Moiseev, in *Proc. of the 5th Intern. Conf. on Instrumentation for Colliding Beam Physics*, p. 380 (World Scientific, Singapore, 1990).
[186] A. E. Kiryunin and A. M. Moiseev, Preprint 91-11, IHEP, Serpukhov (1991) [in Russian].
[187] A. E. Kiryunin and A. M. Moiseev, Yad. Fiz. **56**, 186 (1993) [Sov. J. Nucl. Phys. **56**, 1099 (1993)].
[188] A. E. Kiryunin and A. M. Moiseev, Yad. Fiz. **56**, 195 (1993) [Sov. J. Nucl. Phys. **56**, 967 (1993)].
[189] D. Denegri, in *Proc. of the Large Hadron Collider Workshop*, Aachen (1990).
[190] G. Pancheri *et al.*, Preprint CERN-PPE/92-001, CERN, Geneva (1992).

Translated by Patricia A. Millard